The Growing Little Brain: Cerebellar Functional Development from Cradle to School

Wenjiao Lyu[1,2,†], Kim-Han Thung[1,2,†], Khoi Minh Huynh[1,2,†], Li Wang[1,2], Weili Lin[1,2], Sahar Ahmad[1,2], & Pew-Thian Yap[1,2,✉]

[1]*Department of Radiology, University of North Carolina, Chapel Hill, NC, USA*
[2]*Biomedical Research Imaging Center, University of North Carolina, Chapel Hill, NC, USA*

Despite the cerebellum's crucial role in brain functions, its early development, particularly in relation to the cerebrum, remains poorly understood. Here, we examine cerebellocortical connectivity using over 1,000 high-quality resting-state functional MRI scans of children from birth to 60 months. By mapping cerebellar topography with fine temporal detail for the first time, we show the hierarchical and contralateral organization of cerebellocortical connectivity from birth. We observe dynamic shifts in cerebellar network gradients, which become more focal with age while maintaining stable anchor points similar to adults, highlighting the cerebellum's evolving yet stable role in functional integration during early development. Our findings provide the first evidence of cerebellar connections to higher-order networks at birth, which generally strengthen with age, emphasizing the cerebellum's early role in cognitive processing beyond sensory and motor functions. Our study provides insights into early cerebellocortical interactions, reveals functional asymmetry and sexual dimorphism in cerebellar development, and lays the groundwork for future research on cerebellum-related disorders in children.

The cerebellum's contributions to human language, emotional regulation, attention control, cognition, and working memory, beyond its widely acknowledged role in motor functions, have garnered increasing attention in recent years[1–3]. These diverse functions are believed to result from the cerebellum's interaction with the cerebrum, positioning the cerebellocortical system as one of the most crucial circuits in the human brain[4]. Evolutionary anthropologists suggest that brain expansion in primates, including humans, is driven by the selective modular expansion of the cerebellocortical system[5]. Notably, compared to other primates, key regions associated with cognition in the human cerebellocortical system expand at the highest evolutionary rates[6], indicating that this system may play a pivotal role in the evolution of human brain functions and may offer critical clues on the formation of higher-order cognitive functions in humans. Numerous studies, including those involving non-human primate experiments and human neuroimaging research, have confirmed the connections between the cerebellum and cortex[7]. Additionally, clinical studies[8,9] have shown that damage to the connections between the cerebellum and cortex during development may lead not only to cerebellar abnormalities but also impairment of cerebral cortical development, underscoring the importance of cerebellocortical connectivity in early neurodevelopment. However, knowledge about typical cerebellocortical connectivity and its developmental patterns during the early stages of human life remains lacking.

Children progress through several distinct stages in early childhood—neonatal, infancy,

✉ Corresponding author: Pew-Thian Yap (ptyap@med.unc.edu)
† Equal contribution

toddlerhood, and preschool—each marked by rapid motor and cognitive development. In the neonatal stage, children develop basic reflexes and motor responses, such as grasping, head movements, and recognizing their mother's voice. As they transition into infancy, they begin to acquire more complex motor skills, like rolling, sitting, and standing, while gradually displaying higher-order functions like recognizing familiar faces and objects, using simple gestures, and beginning to speak. The toddler stage sees children mastering walking, running, jumping, and throwing, which require coordination, balance, and motor planning. Additionally, they also experience a wider range of emotions, imitate behaviors, and increasingly use language for communication[10–15]. During the preschool years, children further refine these skills and begin to develop fine motor abilities, like drawing, as well as higher-order cognitive functions such as counting, categorization, language development, and storytelling[15,16]. The rapid development of these higher-order functions, particularly before school age, distinguishes humans from other mammals. This intense developmental period has prompted researchers to study how the cerebellum's unique connection to the cerebral cortex supports these advanced abilities.

The development of these motor and cognitive skills is supported by the maturation of neural substrates in the brain after birth, involving processes such as synaptogenesis (formation of new synapses), myelination (insulation of nerve fibers), programmed cell death (apoptosis), and synaptic pruning (removal of unnecessary synapses). These processes occur at different rates across various brain regions during early childhood[17,18]. For example, the visual cortex, which processes sensory input, matures earlier than the prefrontal cortex, which is associated with decision-making and higher cognitive functions[17]. This difference in developmental timing shows that sensory and association regions—key components of the brain's hierarchical organization—do not mature simultaneously. As a result, the organization and strength of cerebellocortical connections—the pathways linking the cerebellum and the cerebral cortex—are likely to differ significantly between children and adults. Understanding these differences can provide insights into how the brain supports the rapid development of complex motor and cognitive abilities during early childhood.

Over the past decade, functional magnetic resonance imaging (fMRI) has been used to study the functional connectivity between the cerebellum and cortical networks. Advances in this field have revealed the macroscale functional organization of the adult cerebellum based on its connections with cortical regions. Key findings include but are not limited to the cerebellum's functional division into primary sensorimotor and supramodal zones[19]; its contralateral connectivity with the cerebral cortex[20]; the presence of multiple topographically organized somatomotor representations[20]; the involvement of cerebellar subregions in both integrative and segregative functions[21]; the contribution of phylogenetically recent regions, Crus I and Crus II, to connections with higher-order cognitive networks[22]; and a functional hierarchy along the central axis of motor and non-motor organization in the cerebellum[23–25]. Additionally, detailed functional mapping of the cerebellum has been achieved at both the group[20] and individual[26] levels.

Despite these advances in understanding cerebellocortical connectivity in adults, research on these connections in young children is still limited[27,28]. Bridging this gap is essential for understanding abnormalities in cerebellocortical connectivity associated with early-onset disorders such as autism spectrum disorder (ASD) and attention deficit hyperactivity disorder (ADHD)[29–34]. Several fundamental questions about early cerebellar development remain unan-

swered:

- When does the cerebellum first begin to contribute to higher-order functions?
- How mature is the cerebellum in terms of its primary motor functions at different developmental stages?
- At what age do children's cerebellar functions resemble those of adults?
- How does cerebellum development differ between male and female children?
- Is there a difference in cerebellar development between the left and right hemispheres, and if so, when does this lateralization commence?
- What is the spatiotemporal pattern of early cerebellar development?
- How does the functional hierarchy of the cerebellum evolve throughout early development?

To answer these questions, we mapped the connectivity patterns between the cerebellum and cerebral resting-state functional networks (RSNs) in children from birth to 60 months, using over 1,000 fMRI scans from 270 participants in the Baby Connectome Project (BCP)[35]. We examined the development and organization of cerebellocortical connectivity over time, focusing on the establishment and timing of higher-order network connections. Additionally, we explored spatiotemporal patterns, lateralization, and sex differences in cerebellocortical connectivity, contributing to a broader understanding of this critical period of early development.

RESULTS

Using independent component analysis, we selected 30 out of 40 RSNs for full coverage of the cerebral cortex. Based on these RSNs, we determined cerebellocortical functional connectivity through partial correlation analysis with the cerebellum. These 30 RSNs were categorized into eight large-scale networks: Sensorimotor Network (SMN), Auditory Network (AUD), Visual Network (VIS), Salience Network (SN), Ventral Attention Network (VAN), Default Mode Network (DMN), Executive Control Network (ECN), and Dorsal Attention Network (DAN) (Figure 1). Each RSN was named according to its affiliation with a large-scale network and its predominant location in the brain (Table S1). To clarify the principles of cerebellocortical organization, we grouped the SMN, AUD, and VIS as primary networks, and the SN, VAN, DMN, ECN, and DAN as higher-order networks, depending on whether they are primarily engaged in sensory and motor functions or higher-order cognitive functions.

Cerebellocortical Connectivity We first verified the veracity of our framework in capturing the cerebellar functional organization by localizing the sensorimotor representations of the foot, hand, and tongue[20,26]. We evaluated the functional connectivity between the SM-Foot, SM-Hand, SM-Tongue and the cerebellum and observed that sensorimotor representations in the cerebellum during early childhood exhibit organizational characteristics similar to those in adults. Specifically, in the anterior lobe, the representation is inverted, with the foot anterior to the hand and tongue, whereas in the posterior lobe, the representation is upright, with the tongue anterior to the hand and feet (Figure 2a). Using the spatially unbiased atlas template (SUIT) software package developed by Diedrichsen and colleagues[36], we confirmed that the SMN representations are situated at expected positions on the flat map (Figure 2b), gauging based on lobular dermacation (Figure 2c). Subsequently, we generated network-specfic flat maps (Figure 3 and Figure S2)

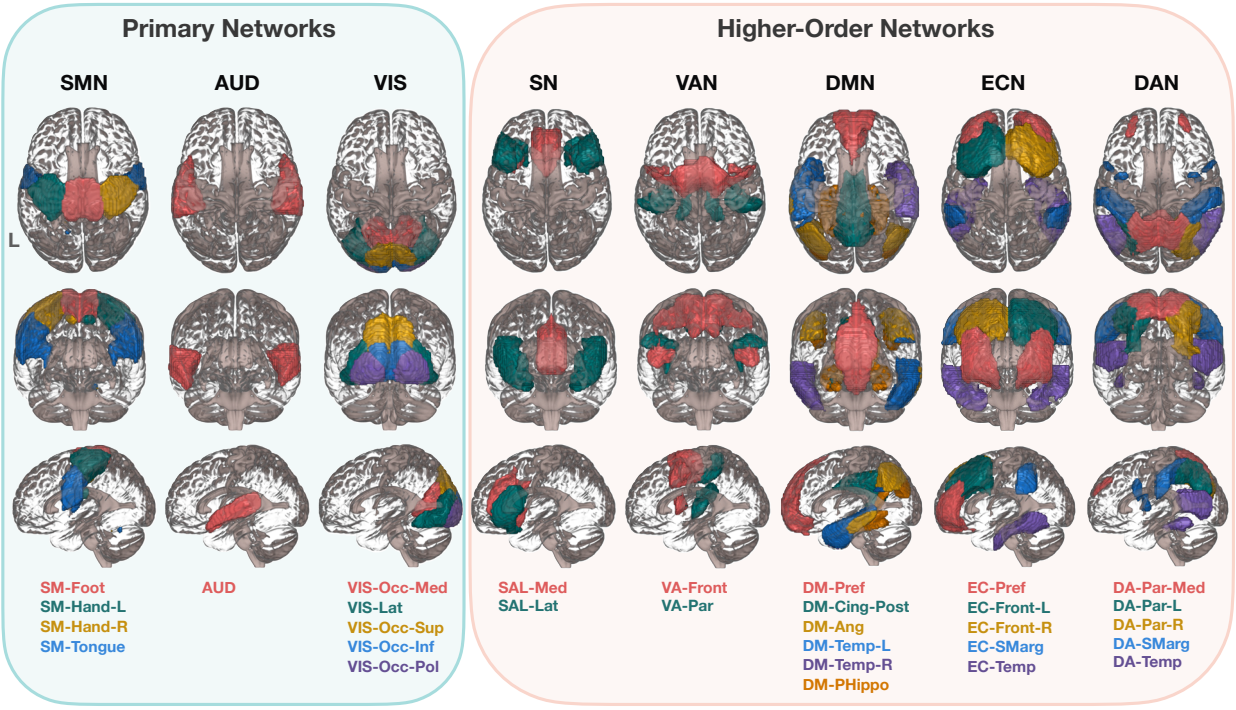

Fig. 1 | **Cortical networks.** Except for the VIS and the DAN, which are presented from superior to inferior, posterior to anterior, and left to right, all networks are displayed from superior to inferior, anterior to posterior, and left to right. SMN: sensorimotor network; AUD: auditory network; VIS: visual network; SN: salience network; VAN: ventral attention network; DMN: default mode network; ECN: executive control network; DAN: dorsal attention network; SM: sensorimotor; L: left; R: right; Occ: occipital; Med: medial; Lat: lateral; Sup: superior; Inf: inferior; Pol: pole; SAL: salience; VA: ventral attention; DM: default mode; Pref: prefrontal; Cing: cingulate gyrus; Post: posterior; Ang: angular gyrus; Temp: temporal; PHippo: parahippocampus; EC: executive control; Front: frontal; SMarg: supramarginal gyrus; DA: dorsal attention; Par: parietal.

and connectivity trajectories (Figure S3) across ages for spatial and temporal characterizations of cerebellocortical connectivity.

For primary networks (Figure 3, Primary Networks), heightened connectivity was observed between several cerebellar regions, encompassing Lobules I-VI, and VIII, and the SMN in early childhood, in line with previous studies on adults[20,26,38]. Specifically, Lobules I-V, the lateral aspect (away from the vermis) of Lobule VIIIb, and Vermis IV-VIII exhibit robust connectivity with SM-Foot. Lobules V-VI and the medial aspect (towards the vermis) of Lobule VIII exhibit strong connectivity with SM-Hand. As expected, the right cerebellum exhibits more pronounced connectivity with left SM-Hand, and vice versa. Additionally, Lobule VI and the medial aspect of Lobule VIIIb exhibit strong connectivity with SM-Tongue. Interestingly, unlike previous studies focused on adults, connectivity between the cerebellum and AUD can be observed in early childhood, particularly from birth to 12 months of age, albeit appearing disorganized and diffuse. We also identified robust connectivity between the VIS and multiple cerebellar regions (including Lobule VI, Lobule I, and the vermis), encompassing a broader spatial extent than previously

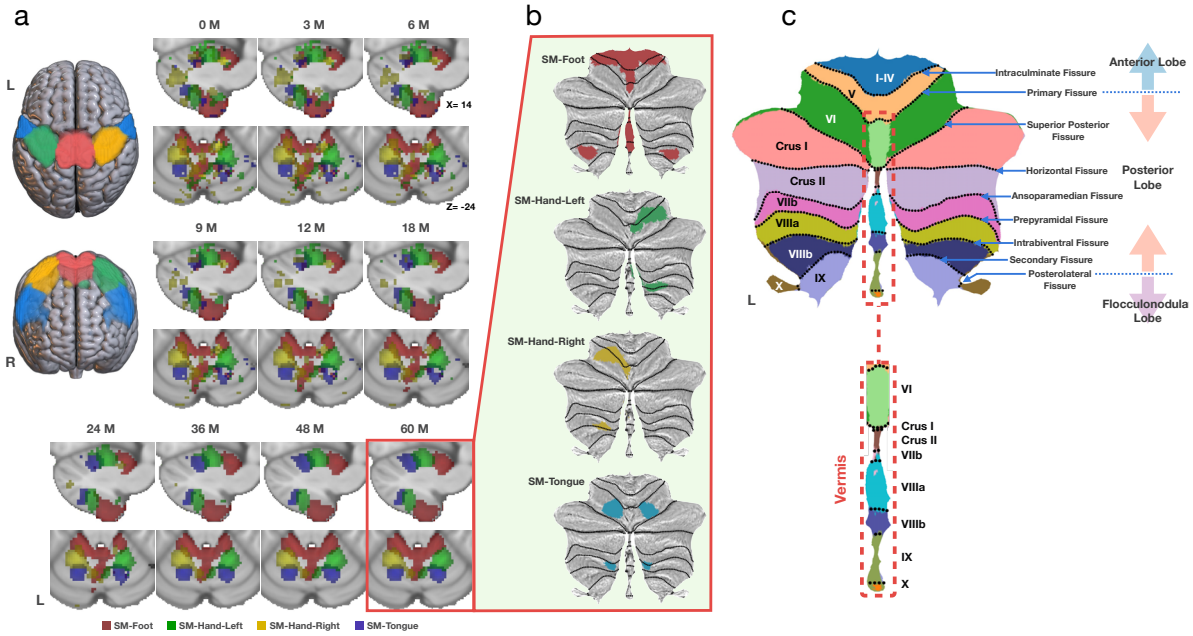

Fig. 2 | Representations of sensorimotor networks. a, Sensorimotor networks and their representations in the cerebellum across age in the MNI space with threshold set at $z = 0.8$. **b**, Flat maps of the sensorimotor representations in the cerebellum at 60 months with threshold set at $z = 0.8$. **c**, Lobular, fissural, and lobar annotation on the cerebellar flat map[36,37].

reported in the literature[20,26,39]. Cerebellar regions with strong connectivity to the VIS-Occ-Med shifted from Lobules V-VI to the inner aspect of Lobule VI and the Vermis VI-VII starting at 36 months. Additionally, we noted an obvious decrease in connectivity between the cerebellar Lobule VI, Crus I, and the vermis with VIS-Occ-Sup from 18 months (Figure S2, Primary Networks), potentially indicating network specialization refinement.

Consistent with prior research on adults, cerebellar regions exhibiting heightened connectivity between higher-order networks are primarily located in Lobules VI, Crus I, Crus II, IX, and X (Figure 3 and Figure S2, Higher-Order Networks). Despite the cerebellum's typically weak and diffuse connectivity with most higher-order networks, strong connections were observed between the cerebellum and certain higher-order RSNs such as DM-PHippo, EC-Pref, bilateral EC-Front, and EC-Temp, which were evident even at birth. Additionally, a trend of predominant contralateral connectivity was observed between the cerebellum and ECN-Front. Specifically, the right cerebellum is predominantly connected with left ECN-Front, whereas the left cerebellum is predominantly connected with right ECN-Front. The cerebellum generally exhibits stronger connectivity with primary networks compared to higher-order networks, especially during the first year of life, as demonstrated by the trajectories of the 99th percentile connectivity (Figure S3a). Biweekly growth rates indicate that connectivity between the cerebellum and the SM-Tongue and VIS-Lat increases with age, while connectivity with most primary networks remains stable or declines. Conversely, connectivity between the cerebellum and most higher-order networks tends to increase with age (Figure S3b). Together, these findings reveal dynamic spatial and strength changes in cerebellar connectivity with RSNs during early childhood and highlight dif-

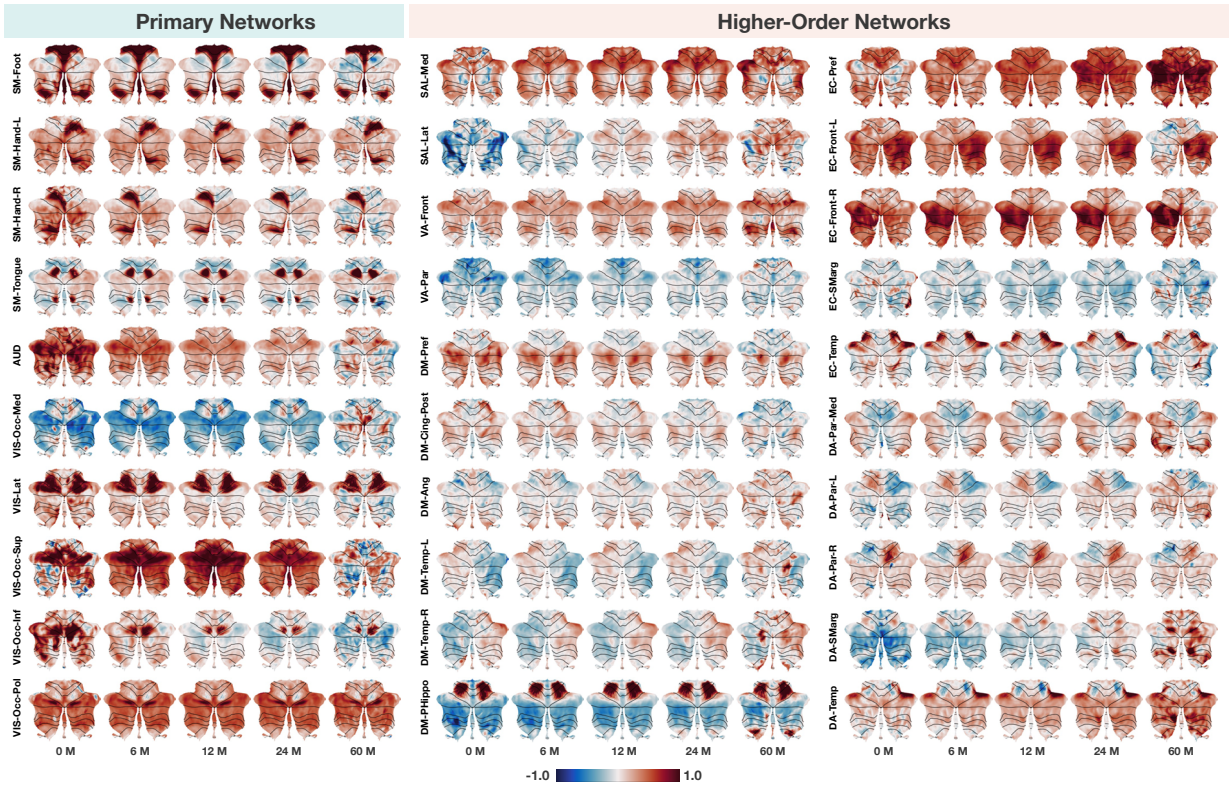

Fig. 3 | **Cerebellar functional flat maps.** Spatiotemporal patterns of connectivity (z-transformed) between the cerebellum and primary networks and higher-order networks at birth, 6 months, 12 months, 24 months and 60 months. Values beyond -1.0 to 1.0 are capped for clarity.

fering developmental trends between RSNs within the same large-scale brain network and the cerebellum.

Cerebellar Functional Topography To better capture the spatiotemporal evolution of cerebellocortical connectivity across early childhood, we employed a winner-take-all approach to identify the network with the strongest connection to each cerebellar voxel[20,27,43,44], generating parcellation maps at three levels of granularity: (i) coarse granularity with two networks (primary and higher-order networks), (ii) medium granularity with eight networks (large-scale networks), and (iii) fine granularity with thirty networks (resting-state networks) (Figure 4a).

At a coarse granularity (Figure 4a, first row), regions in the posterior cerebellar lobe, particularly Crus I and Lobule VIII, connected to primary networks shrink with age, while those in the anterior lobe expand and become more focal. In contrast, posterior lobe regions linked to higher-order networks expand with age. Given that primary networks align with cortical sensory regions, while higher-order networks align with association regions, these findings suggest a developmental hierarchy stratified by the sensory-association (S-A) axis.

At medium granularity (Figure 4a, middle row), regions in Lobule I-VI connected to the

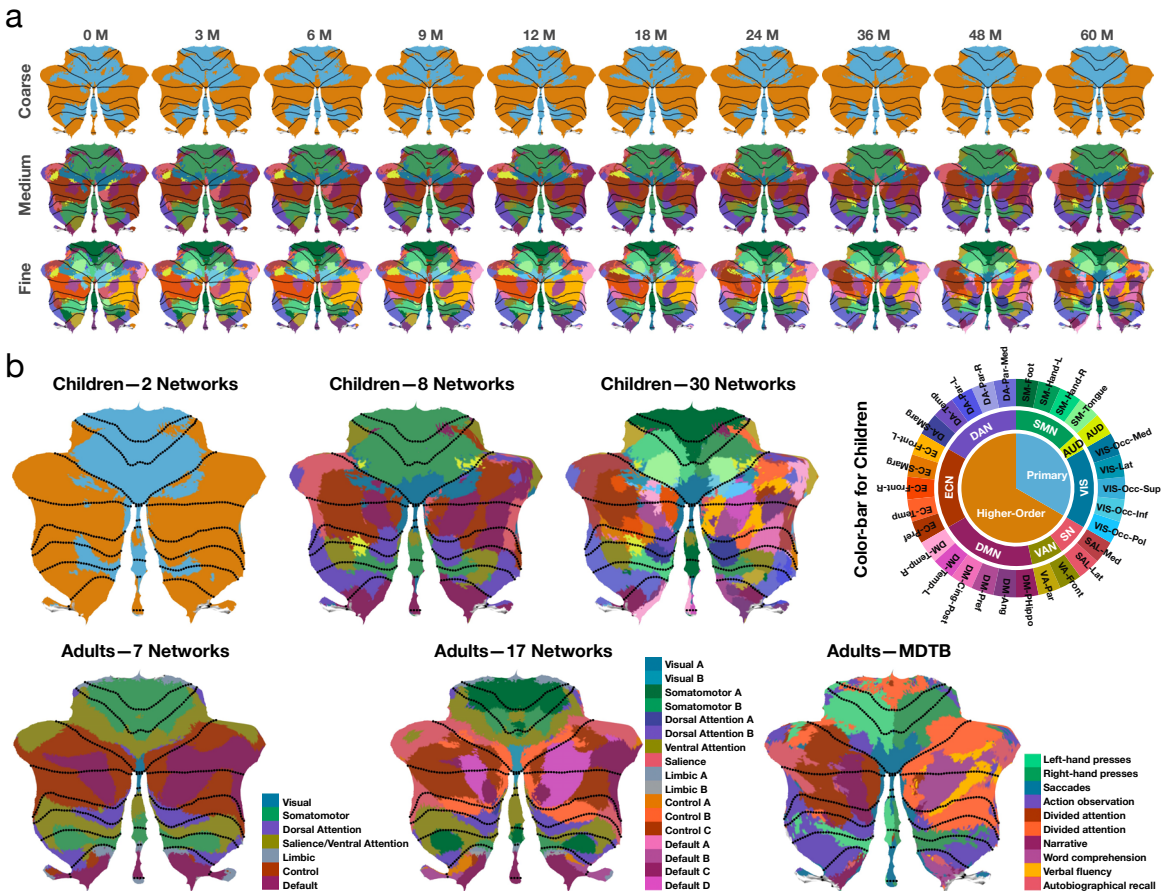

Fig. 4 | **Comparison of parcellation maps between children and adults.** **a**, Spatiotemporal patterns of cerebellar functional topography in early children at coarse, medium and fine granularity. **b**, Parcellation maps for children at 60 months, Buckner et al.'s 7 and 17 cerebellar resting-state networks[40], and the MDTB[41] parcellation map for adults.

SMN remain relatively stable throughout early childhood, whereas regions in Lobule VIII connected to the SMN gradually shrink. With development, cerebellar regions connected to the AUD shift from Crus I to Lobules VI and VIII starting from 24 months. Initially, most cerebellar regions connected to the VIS are located in Crus I. However, as age increases, the areas of Crus I connected to VIS decrease, and by 60 months, the cerebellar regions connected to VIS are mainly concentrated at Vermis VI. Throughout early childhood, Crus I, Crus II, and Lobule VIIb are predominantly connected to the SN, ECN, and DMN, while the lateral aspect of Lobule VIII is primarily connected to the DAN. Additionally, Lobule IX is connected to the VAN and DMN before 24 months; however, after 24 months, it is primarily connected to the DMN.

Functional parcellation at fine granularity (Figure 4a, bottom row) provides a more detailed depiction of the topography of each RSN in the cerebellum, capturing subtle spatiotemporal changes that might be overlooked at medium granularity. For example, at medium granularity, Crus II is primarily connected to the ECN and DMN throughout early childhood. However, at fine granularity, Crus II is predominantly connected to EC-Front and DM-Pref in newborns but

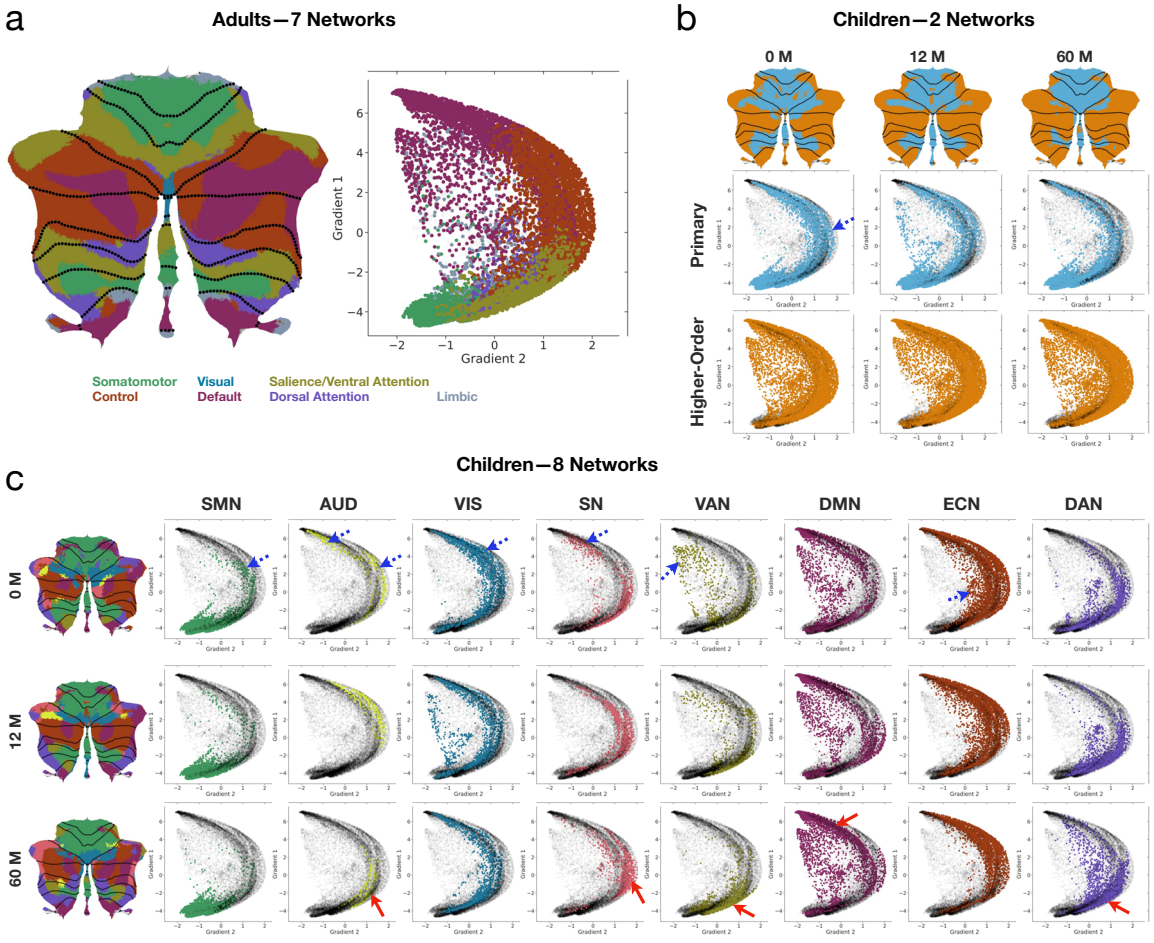

Fig. 5 | **Functional gradients.** **a**, Cerebellar functional gradients in adults[40,42]. **b**, Functional gradients of primary and higher-order networks at birth, 12 months, and 60 months. **c**, Network-specific functional gradients at birth, 12 months, and 60 months. Gradient maps were generated using LittleBrain[42], with each point representing a cerebellar voxel in the MNI space. Regions marked by blue dashed arrows on the gradient maps indicate areas where network points decrease or disappear with age, while regions marked by red solid arrows indicate areas where network points increase with age.

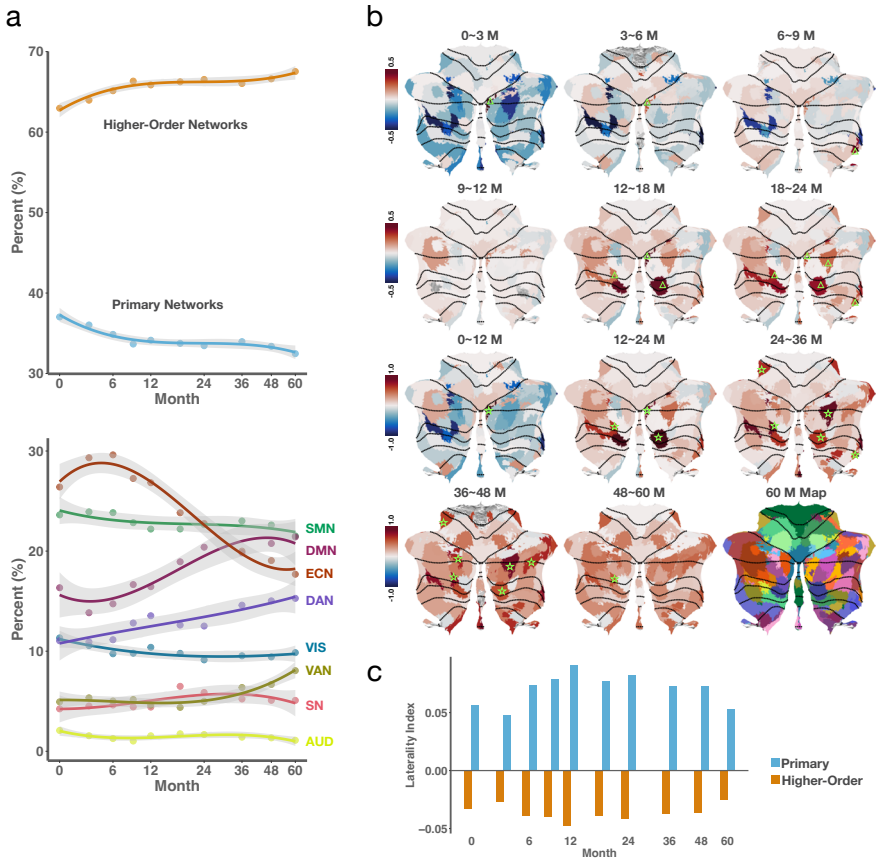

Fig. 6 | **Developmental patterns of cerebellar functional topography. a**, Trajectories of network-specific volume fractions at coarse granularity (top row) and medium granularity (bottom row). The gray shaded area represents the 95% confidence interval for each trajectory. **b**, Spatial maps of changes in 99th percentile cerebellocortical connectivity, based on fine granularity parcellation map at 60 months, for various age intervals. Triangles in the first two rows mark regions with connectivity increases over 20%, whereas stars in the last two rows mark increases over 50%. **c**, Laterality of primary networks and higher-order networks from 0 to 60 months, with laterality index above 0 signifying left lateralization and below 0 signifying right lateralization.

becomes increasingly connected to EC-Pref, DM-Cing-Post, DM-Temp, and DM-Ang as development progresses. Moreover, the fine-granularity parcellation revealed characteristic contralateral cerebellar connectivity with cortical networks, which extends beyond the SMN-related RSNs to other RSNs. For instance, the right cerebellum tends to connect to SM-Hand-L, DM-Temp-L, EC-Front-L, and DA-Par-L, whereas the left cerebellum tends to connect to SM-Hand-R, DM-Temp-R, and EC-Front-R. Notably, RSNs within the same large-scale network are often topographically adjacent in the cerebellum, even if they are spatially distant in the cerebral cortex. For example, DM-Temp-L, DM-Temp-R, and DM-Pref, which belong to the same large-scale network, the DMN, are topographically non-adjacent in the cortex but are adjacent in the cerebellum at 60 months, highlighting the cerebellum's pivotal role in integrating brain function[27,45].

We also compared the cerebellar functional topography maps obtained from 60-month-old

children with Buckner et al.'s cerebellar resting-state networks[40] and the multidomain task battery (MDTB) cerebellar parcellation maps of adults (Figure 4b). Note that the MDTB parcellation map, derived from a set of tasks[41], is labeled according to each region's most defining function, although the region may be assocaited with multiple functions. At 60 months, the cerebellar functional topography of primary and higher-order networks in children exhibits a distinct hierarchical organization (Figure 4b, Children – 2 Networks). Regions predominantly connected to primary networks are mainly situated within Lobules I-VI and the medial aspect of Lobule VIII, wheareas regions dominated by higher-order networks are primarily located in Lobule VII (including Crus I, Crus II, and Lobule VIIb), the lateral aspect of Lobule VIII, Lobule IX and Lobule X, closely resembling the functional organization principles of adults, specifically the pattern of "double motor and triple nonmotor representation"[23,24].

From 24 to 60 months, the cerebellar functional topography of the eight large-scale networks in children (Figure 4a, middle row) progressively mirrors that of the seven resting-state functional networks in adults (Figure 4b, Adults – 7 Networks), reaching high resemblance by 60 months (Figure 4b, Children – 8 Networks) with the following pattern of cerebellocerebral connectivity:

- SMN – Lobules I-VI, medial Lobule VIII, and Vermis VIII.
- AUD – Small regions in Lobules VI and VIII.
- VIS – Crus I and Vermis VI.
- SN – Crus I, Crus II, and Lobule VIIb.
- VAN – Lobule VI and middle Lobule VIII.
- DMN – Crus I, Crus II, Lobules VIIb, IX-X, Vermis IX, and Vermis X.
- ECN – Crus I, Crus II, and Lobule VIIb.
- DAN – Medial Lobule VIIb, lateral Lobule VIII, medial Lobule IX, and Lobule X.

Although the cerebellar connectivity topography in 60-month-old children resembles that of adults, it has not yet fully matured to the adult pattern. Compared to adults, children exhibit greater involvement of the SMN, AUD, and VIS. Interestingly, the cerebellar topography in children also shows increased engagement with the DAN but reduced involvement of the VAN and ECN. These findings suggest a potential shift towards greater functional specialization as the cerebellocortical system matures, reflecting the evolving demands of cognitive and sensorimotor functions during early childhood.

It is perhaps unsurprising that the cerebellar functional parcellation map of 60-month-old children resembles the parcellation map of adults based on resting-state functional networks (Figure 4b, Adults – 7 Networks and 17 Networks). Interestingly, the cerebellar functional parcellation map of 60-month-old children at fine granularity (Figure 4b, Children – 30 Networks) is similar to the adult MDTB parcellation map (Figure 4b, Adults – MDTB). Specifically, the children's SM-Hand-R region largely overlaps with the "Left-hand Presses" region in the adult MDTB map, the SM-Hand-L region overlaps with the "Right-hand Presses" region, the VIS-Occ-Med region overlaps with the "Saccades" region, and the DA-Par-Med region overlaps with the "Action Observation" region. Additionally, the DM-Pref and DM-Temp-R regions correspond with the "Narrative" region, and the DM-Pref and DM-Temp-L regions correspond with the "Word Comprehension" region in the adult MDTB map. These findings suggest that early cere-

bellar functional organization in children is closely linked to specialized tasks, indicating that the cerebellum may develop complex functional mappings earlier than previously thought.

Collectively, these findings demonstrate the dynamic evolution of cerebellar functional topography in early childhood, reflecting the increasing alignment with adult patterns as cognitive development and sensorimotor integration progress.

Cerebellar Functional Gradients We employed LittleBrain[24,42] to generate cerebellar functional gradient maps, complementing the functional parcellation maps by capturing subtle and gradual spatial changes in cerebellar function. LittleBrain creates a two-dimensional map of cerebellar voxels, visualizing functional gradients with each axis representing a principal gradient: Gradient 1, which transitions from primary (motor) to transmodal (DMN, task-unfocused) regions, and Gradient 2, which shifts from task-unfocused (mind-wandering, goal-undirected thought) to task-focused (attentive, goal-directed thought) processing areas. Cerebellar voxels that are adjacent in the gradient map share similar functional connectivity patterns. The gradient map derived from the adult cerebellar functional parcellation[40,42] served as the reference(Figure 5a).

We investigated how functional topography evolves over time by mapping our cerebellar parcellation maps onto the gradient map. At coarse granularity (Figure 5b), the primary networks of children gradually concentrate in lower Gradient 1 and lower Gradient 2 with increasing age.

At medium granularity (Figure 5c), the gradient maps of different large-scale networks evolve differently with age:

- The SMN primarily varies along Gradient 1. With age, the presence of SMN in the high Gradient 1 diminishes. From 9 months onward, the SMN becomes predominantly concentrated in low Gradient 1 and low Gradient 2, in alignment with the SMN gradient pattern observed in adults.
- The AUD initially varies along Gradient 1 and subsequently along Gradient 2. Its distribution shifts from high Gradient 1 to middle Gradient 1 starting from birth to 36 months, and from high Gradient 2 to middle Gradient 2 from 12 to 36 months. The number of points associated with the AUD and the VIS on the gradient maps reduces with age. Given the absence of AUD and the near-absence of VIS in the cerebellar gradient maps of adults, we speculate that the diminishing of AUD and VIS may reflect a shift in cerebellar function from coordinating auditory and visual information to engaging in more advanced cognitive processes during early childhood.
- The VAN primarily varies along Gradient 1. With age, its point distribution in the high Gradient 1 gradually shifts towards the low Gradient 1. From 24 months onward, the VAN is mainly concentrated in low Gradient 1 and slightly higher Gradient 2, resembling the location of VAN in adults.
- The ECN primarily varies along Gradient 2. With age, its point distribution in the low Gradient 2 gradually diminishes, and from 36 months onward, ECN is mainly concentrated in the middle Gradient 1 and high Gradient 2, similar to its position in adults.
- The DMN and the DAN show relatively stable distribution patterns throughout early child-

hood, primarily characterized by an increase and clustering of points in their respective locations.

- The SN primarily varies along Gradient 2. With age, its points in low Gradient 2 gradually reduce while points in high Gradient 2 increase. From 36 months onward, the SN is mainly concentrated in middle Gradient 1 and high Gradient 2. Interestingly, this area intersects with the DMN, VAN, DAN, and ECN, underscoring the SN's pivotal role in network switching[46,47].

The cerebellar gradient maps of large-scale networks covering the entire early childhood period are shown in Figure S7. Together, these gradient maps illustrate that the functional gradients of various large-scale networks evolve dynamically during early childhood. With development, most networks transition from a diffuse to a more focal distribution on the gradient maps, ultimately resembling adult-like patterns. Despite network-specific variations in cerebellar gradient maps during early childhood, the peak concentration locations remain stable and align with adult patterns. This stability highlights consistent functional organization across development, with core areas of network function and connectivity retaining fundamental patterns even as overall activity distributions become more refined.

Temporal Trends We charted temporal changes in cerebellar functional topography based on the volume fraction of each network determined based on winner-take-all parcellation (Figure 6a). At coarse granularity, cerebellar regions connected to primary networks occupy smaller proportions than those connected to higher-order networks throughout early childhood. Notably, from birth to 12 months and 36 to 60 months, regions connected to primary networks shrink, while those connected to higher-order networks expand (Figure 6a, top row).

At medium granularity, regions connected to the primary networks (SMN, AUD, and VIS) decrease, while those connected to higher-order networks (DMN, DAN, and VAN) increase throughout early childhood. An exception is the regions connected to the ECN, which expanded until 6 months, then shrank but remained larger than those connected to any other network until 24 months. From 36 months onward, the regions connected to each network are consistently ranked in size: SMN, DMN, ECN, DAN, VIS, VAN, SN, and AUD (Figure 6a, bottom row). These observations highlight the early interactions between higher-order networks and the cerebellum. Furthermore, the larger cerebellar regions connected to the SMN, DMN, and ECN suggest these networks play significant roles in early development.

Based on the fine-granularity parcellation map at 60 months, we further calculated the growth rates of the 99th percentile cerebellocortical connectivity strength for each RSN across various time intervals (Figure 6b). Persistent positive growth rates are observed in cerebellar connectivity with the SAL-Lat, SAL-Med, and VIS-Occ-Inf during early childhood. Cerebellar connectivity with SAL-Lat increases by over 25% from birth to 3 months and from 3 to 6 months, whereas connectivity with the other RSNs increases by less than 15% during these same periods. Cerebellar connectivity growth rates with most primary networks remain relatively low during early childhood, generally below 20%, except for VIS-Occ-Pol during the first year and SM-Tongue and AUD during the fourth and fifth years, which exceed 20% but do not surpass 50% annually. In contrast, continuous positive annual growth rates are observed in cerebellar

connectivity with higher-order networks, such as SAL-Med, SAL-Lat, EC-Pref, and DA-Par-L. Notably, with the exception of DA-Par-L, the aforementioned RSNs are located in the prefrontal cortex, suggesting that the interaction between the cerebellum and the prefrontal cortex plays a crucial role in early development. Cerebellar connectivity growth rates with higher-order networks in the parietal and temporal lobes may be negative within the first year of life, but from the second year (e.g., EC-SMarg, DA-SMarg, DA-Par-L, and DM-Temp-L) or the third year (e.g., VA-Par, DM-Ang, and DM-Temp-R) onward, many of these connections exhibit strong positive growth rates (over 30% annually), highlighting the asynchronous development of connectivity between different cortical regions and the cerebellum.

We used shorter time intervals to assess cerebellocortical connectivity growth rates during the first two years, capturing subtle changes that longer intervals might miss. For example, while the annual growth rate of DA-Par-L connectivity in the first year was 19.85%, quarterly intervals showed a more nuanced pattern with periods of negative, zero, positive, and subsequent negative growth. The growth rates for all RSNs are reported in Table S2. These results reveal dynamic changes in cerebellocortical connectivity during early childhood, showing how interactions between cerebellar regions and cortical networks evolve over time. This highlights the cerebellum's adaptive role in processing sensorimotor and cognitive information, underscoring its influence on developmental trajectories.

Functional Lateralization The functional lateralization of primary motor and higher cognitive functions in the cerebellum is well established, with cerebro-cerebellar circuits considered to play a crucial role[48]. However, longitudinal research on cerebellocortical connectivity functional lateralization in developing children is currently lacking. To address this gap, we investigated cerebellar laterality with respect to the primary and higher-order networks from 0 to 60 months. Using coarse-granularity parcellation maps, we calculated the laterality indices by determining the number of voxels in the left and right cerebellar hemispheres connected to higher-order and primary networks at each age. We observed consistent rightward lateralization of cerebellar connectivity with higher-order networks and leftward lateralization with primary networks throughout early childhood (Figure 6c), highlighting the distinct lateralization patterns between the cerebellum and these networks during early development. Our findings provide evidence, from the perspective of cerebellocortical connectivity, for functional changes resulting from unilateral cerebellar abnormalities in early life.

Sex Differences Sexual dimorphism in cerebellar gray and white matter volumes has been well-established in children and adolescents. However, research has yet to explore sexual dimorphism in cerebellocortical connectivity during early childhood. To fill this gap, we investigated cerebellocortical connectivity separately in female and male children, aiming to understand how sexual dimorphism may influence cerebellocortical connections from early development.

By examining cerebellocortical connectivity, we found that cerebellar regions exhibiting strong connections with each RSN are generally consistent between female (Figure S4) and male (Figure S5) children. Analysis of the 99th percentile cerebellar connectivity with each RSN revealed that, within primary networks, female children exhibit higher connectivity with SMN-Foot, SMN-Hand-L, SMN-Tongue, and VIS-Occ-Med, but lower connectivity with VIS-Occ-Inf and VIS-Occ-Pol compared to their male counterparts. Within higher-order networks, female

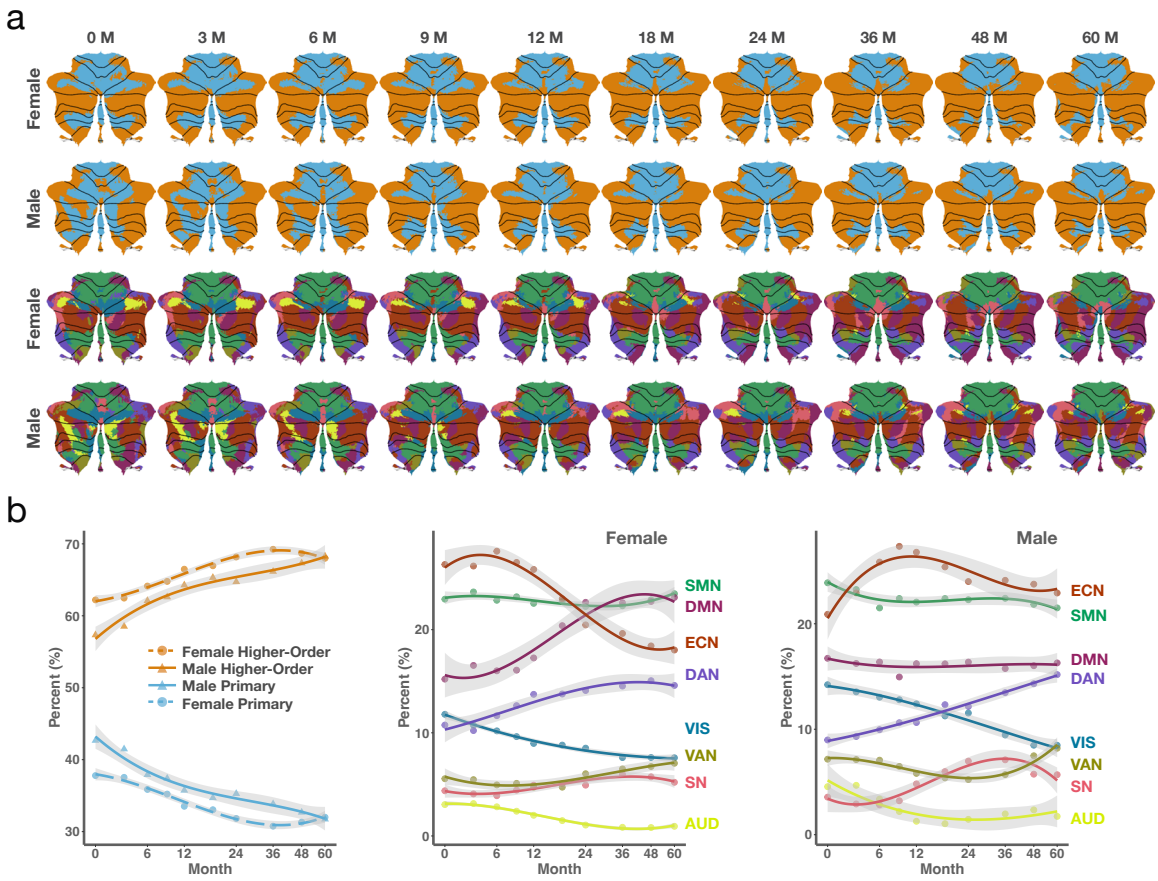

Fig. 7 | **Spatiotemporal patterns of functional topography for female and male children. a**, Parcellation maps for female and male children at coarse granularity (first two rows) and medium granularity (last two rows). **b**, Trajectories of network-specific volume fractions for female and male children at coarse granularity (first column) and medium granularity (second and third columns). The gray shaded area represents the 95% confidence interval for each trajectory.

children demonstrate stronger connectivity with DM-Temp-R, EC-Front-R, DA-Par-Med, DA-Par-L, and DA-Par-R compared to males throughout most of early childhood (Figure S6).

We generated cerebellar functional parcellation maps for female and male children (Figure 7a) to assess whether cerebellar functional topography exhibits sexual dimorphism. It can be observed from the coarse-granularity parcellation maps that the hierarchical organization of primary and higher-order networks is evident in female children throughout early childhood, whereas similar organization in males only becomes apparent after 12 months. The medium-granularity parcellation maps reveal that before 12 months, Lobule IX in both sexes primarily connects to the DMN and VAN. However, after 12 months, Lobule IX in female children primarily connects to the DMN, while in male children it connects more diversely to the ECN, DMN, VAN, and VIS, indicating the regional functional specialization of the cerebellum during early childhood appears less pronounced in males.

We further delineated the temporal trajectories of network volume fractions at both coarse and medium granularity levels (Figure 7b). At coarse granularity, there is an upward trend in cerebellar regions connected to higher-order networks in males from birth to 60 months, whereas in females, there is an increase from birth to 36 months followed by a decline from 36 to 60 months. Cerebellar regions connected to higher-order networks in females remain higher than in males until 48 months, only marginally lower at 60 months (Figure 7b, left column). At medium granularity, cerebellar regions connected to the SMN, ECN, and DMN are consistently the largest, regardless of sex. In female children, regions connected to the ECN are the largest before 18 months, but thereafter, regions connected to the DMN and SMN both surpass those connected to the ECN (Figure 7b, middle column). In male children, excluding at birth, regions connected to the ECN are the largest, followed by those connected to the SMN and DMN (Figure 7b, right column). This pattern suggests a sexually dimorphic developmental trajectory in cerebellocortical connectivity, where male children exhibit a persistently stronger cerebellar connection to the ECN, potentially reflecting a more pronounced development of executive functions. Conversely, female children display a stronger cerebellar connection to the DMN as they grow, which may indicate earlier development of introspective and self-referential processing functions.

We generated the cerebellar functional gradient maps for eight large-scale networks during early childhood, separately for female (Figure S8) and male (Figure S9) children. As expected, the cerebellar functional gradients of female and male children show overall consistency with age, but sexual dimorphism persists for certain networks. For instance, with increasing age, both female and male children show lowering Gradient 1 and Gradient 2 for the AUD, along with a reduction in the number of associated points. However, from 12 months onward, the decrease in gradient values and the number of points of AUD is more pronounced in female children compared to male children. Additionally, after 12 months, the DMN gradient maps for female children exhibit more voxels and higher Gradient 1 than those of male children, with DMN gradient regions in females more closely resembling adult patterns. These observations suggest that the functional gradients of large-scale networks in females may approach adult-like patterns earlier than in males. Collectively, these findings underscore the importance of considering sex differences in cerebellocortical connectivity to better understand early cerebellar development.

DISCUSSION

While extensive research has clarified the motor and cognitive functions of the cerebellum in adults[23,40,49,50], these roles remain poorly understood in early childhood—a critical period of rapid neural development. This stage, marked by ongoing synaptic pruning[18,51], a vital process that refines and reorganizes neural connections in response to developmental changes and external stimuli, offers a key window of opportunity for intervention in neurodevelopmental disorders. Our study aimed to fill this gap by examining cerebellar connectivity with cortical networks and mapping its functional topography in children aged 0 to 60 months. Our findings show that cerebellar connectivity to higher-order networks is present at birth and generally strengthens throughout early childhood. We identified the contralaterality and hierarchical organization patterns of cerebellocortical connectivity in early childhood, and revealed that cerebellar functional topography begins to exhibit an adult-like pattern at 24 months and becomes increasingly similar over time. By mapping cerebellar functional gradients, we observed that the

dispersed gradients of large-scale networks within the cerebellum during early childhood dynamically shift toward a more focal pattern with age, while maintaining stable anchor positions, similar to those observed in adults. We observed lateralized patterns of cerebellar connectivity, with higher-order networks being right-lateralized and primary networks being left-lateralized, further highlighting the cerebellum's functional asymmetry. We identified notable sexual dimorphism in both the organization and development of cerebellocortical connectivity, highlighting the differential trajectories of cerebellar functional maturation between males and females. These findings emphasize the early development of cerebellocortical connectivity, its role in neurodevelopment, and its potential influence on cognitive and motor outcomes, offering guidance for future research and clinical intervention in cerebellar dysfunction.

The cerebellum's role in motor control and sensory modulation is well-established in humans[52] and other species[53], coordinating complex activities like skilled finger movements, eye positioning, and trunk and limb control. It is also crucial for motor learning[54], essential for acquiring and refining motor skills. Damage to the cerebellum's auditory and visual regions reduces accuracy in auditory- and visual-evoked orienting behaviors[53], highlighting its role in sensory processing. Cerebellar injury can impair visual target tracking[55] and motion detection[56], underscoring the cerebellum's importance in sensory-motor integration. Despite these findings, few studies[27,57] have examined cerebellum-motor cortex connectivity in young children, and neuroimaging evidence of cerebellar connections with the AUD and VIS is limited. Our study confirms the developing cerebellum connects with both the SMN and sensory regions like the AUD and VIS. Notably, the proximity of the auditory cortex to the sensorimotor cortex has often led to its distinct cerebellar connections being overlooked. Recent research[58] identified unique cerebellar connections to the auditory cortex, separate from those to the SMN. Our study adds to this understanding by showing that cerebellar connectivity with the AUD differs from the SMN not only in strength but also in developmental patterns, underscoring the cerebellum's distinct role in auditory processing during early development. Moreover, we found strong cerebellar connectivity with the VIS in early childhood, in stark contrast to the substantially weaker connectivity seen in adults. In adults, most cortical areas show cerebellar homology, but functional connectivity between the visual cortex and cerebellum is limited[20]. The few connections between the cerebellar vermis and VIS in adults[26,39] are far less pronounced than the extensive connectivity seen in children. This difference may reflect the dominance of visual, auditory, and sensorimotor cortical hubs in early childhood[59].

While there is consensus on the existence of connectivity between the cerebellum and primary networks, uncertainty remains regarding its connectivity with higher-order networks during early childhood. Research in this area is limited, yielding contradictory findings. One study found no such connectivity in infancy[27], while another identified cerebellar connections to higher-order regions, including the prefrontal cortex, anterior cingulate cortex, and insula[60]. This highlights the complexity of cerebellocortical interactions and the necessity for further investigation. A recent study[61] provides critical insight into these interactions, revealing that neonatal cerebellar injury can disrupt the development of higher-order cortical regions. Beyond motor impairments, neonates with isolated cerebellar injuries may exhibit cognitive, language, and social behavioral abnormalities during development[62,63], suggesting crucial connectivity between the cerebellum and higher cognitive networks during early development.

Infant learning was perceived as a passive accumulation of sensory experiences, predominantly associated with the sensory and motor cortex. However, emerging research[64] posits that infants are intrinsically motivated for active learning, with involvement from regions such as the prefrontal cortex. Our study corroborates this view by revealing widespread cerebellar connectivity with higher-order networks during early childhood. Connectivity with higher-order networks is weaker than with primary networks but generally strengthens with age. Notably, specific higher-order networks, especially the ECN located in the frontal and prefrontal regions, exhibit robust connectivity with the cerebellum from birth. This finding is consistent with our previous research[65], which highlighted strong structural connections between the cerebellum and the superior frontal gyrus—one of the key regions of the ECN. Our findings confirm that the connectivity between the cerebellum and higher-order networks is established early in life and may play a crucial role in shaping cognitive and behavioral functions during childhood, potentially influencing the developmental trajectory of these networks into adulthood. This early interaction may shed light on the underlying mechanisms of cognitive disorders such as ASD and ADHD, which are linked to abnormal cerebellar connections with higher-order networks[29–34], offering new insights into how cerebellar development affects later cognitive functions.

The contralateral organization of cerebellar functional topography with the motor and prefrontal cortices is well-established in adults[19,20]. Our findings extend this organization to early childhood, reinforcing the existence of the cross-hemispheric cerebrocerebellar loop[66]. Identifying this loop in early childhood may provide insights into contralateral developmental abnormalities in the cerebellum following unilateral cerebral damage in infancy, possibly due to remote trans-synaptic effects[8]. Beyond contralaterality, another key feature we observed is the hierarchical organization of primary and higher-order networks within the cerebellum, closely aligned with the S-A axis[67]. Extending from primary sensorimotor and visual regions to higher-order association areas[68,69], the S-A axis reflects a fundamental principle of hierarchical cortical organization, with spatiotemporal pattern of cortical maturation proceeding hierarchically along this axis[68,70]. While the hierarchical organization along the S-A axis is well established for the cortex, corresponding research on the cerebellum remains limited. Guell et al.[24] identified functional gradients in the cerebellum that mirror the cortical hierarchy, revealing a dual motor and triple nonmotor organization. However, unlike the S-A axis of cerebellocerebral connectivity in adults[24,71], where gradient boundaries are near the superior posterior, prepyramidal, and secondary fissures, the first gradient boundary at birth occurs at the horizontal fissure. This boundary shifts gradually, reaching the superior posterior fissure by 60 months, with the second and third gradient boundaries resembling those in adults at the prepyramidal and secondary fissures. These findings indicate that the cerebellum's hierarchical organization of primary and higher-order functions is present from birth and progressively aligns with adult functional organization along the S-A axis. This alignment likely reflects the cerebellum's early integration into broader cortical systems, offering critical insights into the cerebellocerebral connectivity patterns that support cognitive and motor development in early childhood.

In the past decade, research on the functional connectivity gradients of large-scale networks in the cerebral cortex has gained considerable attention[72–74]. A recent study[75] mapped changes in cortical functional gradients across the entire human lifespan from cradle to grave. However, investigations on cerebellar functional gradients have predominantly focused on adults, represented primarily by the seminal work of Guell and colleagues[24,25,42]. The study of cerebellar gra-

dients of large-scale networks in children, in particular, remain largely unexplored. For the first time, we mapped the functional gradients of large-scale networks in the cerebellum throughout early childhood, revealing how these gradients evolve during this critical period of brain development. In adults, distinct patterns of cerebellar gradients have been observed[24,25,42]: the motor network, ECN, and DMN occupy low, middle, and high positions on Gradient 1, respectively. The VAN and DAN are positioned along Gradient 1 away from the DMN, with the ECN situated between the VAN/DAN and DMN, acting as a mediator. Gradient 2 is thought to relate to task load, with low Gradient 2 corresponding to low task load networks such as the motor network and DMN, and high Gradient 2 to task-positive networks, including the VAN, DAN, and ECN. Not surprisingly, the cerebellar functional gradients at birth do not fully replicate the patterns observed in adulthood. Instead, these networks exhibit more dispersed gradients that gradually become more focal, converging towards an adult-like pattern as children mature. By 60 months, these gradients resemble those in adults, but the exact age of full cerebellar functional gradient maturity requires further research across different age groups. Since similar functions occupy adjacent gradient positions[73], the progressive focalization of these gradients reflects functional specialization. Notably, despite dynamic changes in cerebellar gradients during early childhood, the anchor positions remain stable, mirroring those in adults. This suggests the foundational framework is established at birth and refined with age, likely through synaptic pruning or activity-dependent processes, supporting the idea that early cerebellar organization shapes its mature functional architecture.

The human brain experiences rapid growth in the first two years[76,77], with gray and white matter expansion, myelination, and higher-order function development[17]. Functional networks for verbal skills form in the first year and predict later language and literacy skills[78]. In line with this, our findings show a rapid increase in cerebellar regions tied to higher-order networks, emphasizing the cerebellum's role in early cognitive development. We also observed further expansion of these regions between ages 3 and 5, supporting the importance of prekindergarten education[79,80]. Notably, the cortical networks showing increased connectivity with the cerebellum during early childhood are primarily in the prefrontal cortex, which is responsible for cognitive functions, executive control, attention, emotion, inhibition, self-monitoring, working memory, and language[81,82]. While the prefrontal cortex was once thought to develop late, recent neuroimaging shows it is active as early as three months, particularly in language processing and memory[83–85]. Studies in both non-human primates and humans confirm the prefrontal-cerebellar connection, though evidence in early childhood is limited[86–88]. Our study reveals an asynchronous development pattern in cerebellocortical connectivity. While cerebellar connections with prefrontal RSNs show positive growth in the first year, connections with RSNs in the parietal and temporal regions grow strongly only from the second year.

Studies on cerebellar functional asymmetry suggest that cognitive functions typically exhibit right laterality, while motor functions tend to show left laterality[48]. Consistent with this, our findings indicate that the cerebellum demonstrates rightward lateralization in connection with higher-order networks and leftward lateralization with primary networks throughout early childhood. Clinical studies[89,90] further support this pattern, revealing that damage to the right cerebellar hemisphere can lead to cognitive impairments, including deficits in language and literacy, whereas left cerebellar damage is frequently associated with specific visuospatial impairments and deficiencies in spatial skills. Given that language processing is predominantly lateralized to

the left cortical regions and visual functions are right-lateralized[91,92], the cerebellum's functional lateralization in early childhood may arise from the aforementioned cerebellocortical contralateral organization. These findings highlight the role of lateralization in early neurodevelopment, showing that cerebellocortical connectivity supports both hemispheres, promoting balanced cognitive and motor development essential for effective interaction with the environment.

Sexual dimorphism in human brain structure and function is well documented[93–95]. Sexual differentiation of the human brain is a complex process influenced by genetic, steroid hormone, neurotransmitter, neuropeptide, and enzyme interactions[96], thought to be at least partially established during early development[93]. Although there are currently no reports on sexual dimorphism in cerebellocortical connectivity during development, it has been confirmed through cerebellar volumetric studies of infants, children, adolescents, and adults[97–99]. Our findings add to this body of work by revealing that the cerebellum's hierarchical organization emerges later in male children than in female children, with male children exhibiting less pronounced regional specialization. Notably, before age 5, female children exhibit larger cerebellar regions connected to higher-order networks compared to their male counterparts. We further observed that the cerebellar gradients of large-scale networks in female children align with the adult pattern earlier than male children. These findings, in conjunction with a previous study on cerebellar volumetric development from 5 to 24 years of age[98], showing males reach peak volumes later than females for the entire cerebellum and various lobes (anterior, inferior posterior, and superior posterior), lead us to speculate that the maturation of cerebellocortical functional connectivity, particularly with respect to higher-order networks, may occur later in males. This delay may partly explain the susceptibility of males to early-onset neuropsychiatric disorders[100] such as ASD[101] and ADHD[102], which involve reduced cerebellar connectivity with higher-order networks. In addition, our study indicates that female children exhibit noticeably stronger cerebellar connectivity with the SM-Tongue compared to male children during early childhood. This finding may provide imaging evidence supporting earlier speech production[103] and better verbal performance[104] in female children. Our study underscores the need to explore sexual dimorphism in early cerebellocortical connectivity, as it may impact cognitive and behavioral outcomes. Future research in this direction can clarify sex-specific vulnerabilities and guide interventions for neurodevelopmental and psychiatric conditions.

In summary, we investigated cerebellocortical connectivity during early childhood, spanning from birth to 60 months. Our findings demonstrate the presence of cerebellar connectivity not only with primary networks but also with higher-order networks, even at birth. Our parcellations with fine temporal resolution captured functional topography at different developmental stages, revealed the hierarchical organization of primary and higher-order networks, and suggested an S-A axis of early cerebellar functional development. Furthermore, our study shed light on the lateralization and sexual dimorphism of cerebellar functions. These findings offer insights into early neurodevelopment and may contribute to the diagnosis and monitoring of early-onset cerebellum-related disorders.

METHODS

Participants The data utilized in this study were collected as part of the UNC/UMN Baby Connectome Project (BCP)[35]. After data preprocessing and quality control, the final dataset included 1,001 scans from 270 healthy participants (129 males and 141 females) ranging from birth to 60 months, with up to six longitudinal scans per participant. Parents were fully informed of the study's objectives before providing written consent. Ethical approval for all study procedures was granted by the Institutional Review Boards of the University of North Carolina at Chapel Hill (UNC) and the University of Minnesota (UMN).

Data Acquisition Scans were conducted on children younger than 3 years (0–35 months) while they were naturally asleep, without the use of sedatives. Prior to imaging, all babies were fed, swaddled, and fitted with ear protection. For children older than 3 years (36–60 months), scans were performed while they were either asleep or watching a passive movie[35,105]. All images were acquired using 3T Siemens Prisma MRI scanners (Siemens Healthineers, Erlangen, Gernamy) with 32 channel coils at the Biomedical Research Imaging Center (BRIC) at UNC and the Center for Magnetic Resonance Research (CMRR) at UMN[35]. MRI acquisition parameters are summarized as follows:

- T1 weighted MR images were obtained with a 3D magnetization prepared rapid gradient echo (MPRAGE) sequence: isotropic resolution = 0.8 mm, field of view (FOV) = 256 mm $\times$ 256 mm, matrix = 320 $\times$ 320, echo time (TE) = 2.24 ms, repetition time (TR)= 2400/1060 ms, flip angle = 8°, and acquisition time = 6 min 38 s.
- T2 weighted MR images were obtained with a turbo spin echo (TSE) sequence: isotropic resolution = 0.8 mm, FOV = 256 mm $\times$ 256 mm, matrix = 320 $\times$ 320, TE = 564 ms, TR = 3200 ms, and acquisition time = 5 min 57 s.
- Resting-state functional MRI data were collected using a single-shot echo-planar imaging (EPI) sequence: isotropic resolution = 2 mm, FOV = 208 mm $\times$ 208 mm, matrix =104 $\times$ 104, TE = 37 ms, TR = 800 ms, flip angle = 52°, and acquisition time = 5 min 47 s.

Data Preprocessing fMRI data processing is summarized in Figure S1. The fMRI blood oxygen level dependent (BOLD) data were first minimally preprocessed as follows: (i) Head motion correction using FSL's `mcflirt` function[106], which rigidly registered each fMRI time frame to the a single-band reference (SBref) image and generated the corresponding motion parameter files; (ii) EPI distortion correction using FSL's `topup` function[107,108], which generated a distortion correction deformation field using a pair of reversed phase-encoded FieldMaps; (iii) Rigid registration (degrees of freedom = 6) of SBref to FieldMaps; (iv) Rigid boundary-based registration (BBR)[109] of distortion corrected SBref image to the corresponding T1-weighted (T1w) images, with prealignment using mutual information cost function; and (v) One step sampling by combining all deformation fields and translation matrices above and applying them to the raw 4D fMRI data, resulting in motion and distortion corrected fMRI data in the subject native space (T1w space)[110].

Data Denoising We refined the minimally preprocessed fMRI data to eliminate noise before further analysis. Firstly, we employed detrending to remove slow drift by applying a high pass filter with a cutoff frequency of 0.001 Hz. Next, we utilized Independent Component Analysis-based

Automatic Removal Of Motion Artifacts (ICA-AROMA)[111,112] to address any residual motion artifacts. This process involves performing a 150-component independent component analysis (ICA) on the fMRI data and classifying each component as either BOLD signal or artifact based on high-frequency contents, correlation with realignment parameters (i.e., motion parameters estimated in head motion correction), edges, and CSF fractions. Components classified as artifacts are then non-aggressively removed through regression, retaining signal components sharing variance with artifacts. Following denoising, Gaussian smoothing with a full-width half-maximum (FWHM) of 4 mm was applied. Subsequently, the data were mapped into the MNI space and underwent intensity normalization for a constant mean volume intensity of 10,000.

Quality Control To ensure good data quality, we computed framewise displacement (FD) from motion parameters obtained through head motion correction. Samples with mean Power's FD (absolute sum of motion parameters) exceeding 0.5 mm—a common threshold used in fMRI studies[113]—were excluded. Additionally, we set a limit for Jenkinson's FD[114] (Euclidean sum of motion parameters) at 0.2 mm to further minimize the impact of motion-affected samples. Out of 1,656 preprocessed fMRI samples, 1,493 met the Power's FD criterion, and 1,278 further satisfied the Jenkinson's FD criterion. We then visually evaluated the quality of skull stripping, tissue segmentation, and fMRI-to-T1w image registration, retaining 1,245 with satisfactory quality. The fMRI data in MNI space were categorized based on geometric distortions as "pass" (no or light distortion), "questionable" (light to medium distortion), and "fail" (medium to large distortion). After visual inspection, 1,047 samples were labeled as having "questionable" or better quality, out of which 703 were labeled as "pass". Samples with "fail" quality were excluded from our analysis. We judiciously used the data according to these categories. We computed template spatial maps using only the "pass" labeled data to minimze artifacts in determining meaningful functional networks. We eliminated 46 from the 1,047 initially labeled as "pass" or "questionable" due to erroneous results in partial correlation analysis, resulting in a final total of 1,001 samples for subsequent analyses.

Independent Component Analysis and Network Identification We performed probabilistic group independent component analysis (GICA) exclusively on the "pass" fMRI data to ensure fewer noise-related components, ultimately yielding 40 RSNs, which served as templates for subsequent analyses. Anatomical examination of the template RSNs revealed that 30 were located in the cortex, while 10 were situated in the cerebellum or subcortical areas. We further categorized the 30 cortical RSNs into eight large-scale networks[20,115]: SMN, VIS, AUD, SN, VAN, DMN, ECN, and DAN. The details of these RSNs are presented in Table S1. RSNs within the SMN were named according to major motor functions, while those in other large-scale networks were named based on their anatomical locations. The terms "Left" and "Right" designate the hemisphere (left or right) where each component is situated. Using the template RSNs, we determined the RSNs for each individual based on their denoised fMRI data using dual regression[116]. Gaussian mixture modeling was then applied to each individual RSN to generate activation probability maps, which were employed in a winner-take-all scheme for individualized non-overlapping cortical parcellation.

Cerebellocortical Functional Connectivity Cerebellocortical functional connectivity was computed for each voxel in the cerebellum relative to various cortical functional networks. First, we applied a Butterworth bandpass filter to the BOLD time series, focusing on the low frequency

spectrum of 0.008–0.1 Hz[117,118]. The cerebellum was masked using a cerebellar atlas provided by FSL (cerebellar MNI Flirt Maxprob thr25–2 mm)[119]. To prevent cortical voxels in our analysis from being influenced by neighboring cerebellar voxels, we dilated the cerebellar mask by $8\times8\times8\,\mathrm{mm}^3$ and excluded any cortical voxels within this expanded mask. For each of the 30 cortical RSNs, we computed a representative time series to capture coherent activity within the corresponding cortical mask. This involved calculating the major eigen time series for the denoised BOLD signals of the top 10% positively activated voxels within the cortical mask[19]. The major eigen time series is derived as the first eigenvector using singular value decomposition (SVD), with its sign corrected[120] to match the mean time series of these voxels. Subsequently, we calculated partial correlation scores between the cortical eigen time series and the denoised BOLD signals of each cerebellar voxel within the non-dilated cerebellar mask. These correlations were then converted to z-scores using the Fisher's r-to-z transform, representing cerebellocortical functional connectivity (FC). Thus, for each subject, each cerebellar voxel was associated with 30 cerebellocortical FC values, one for each cortical functional network.

Generalized Additive Mixed Model (GAMM) Fitting We fitted a generalized additive mixed model (GAMM) to the cerebellocortical FC of each voxel using the "gamm4" package in R[121]. The model included a smooth term of age and random effects of subject ID and scan site: $Y \sim s(\text{age}, k = 10) + (1|\text{SubjectID}) + (1|\text{SiteID})$, where $s(\cdot)$ denotes the smooth term and $(1|\cdot)$ models the random effects. The number of basis functions, k, is determined empirically to slightly exceed the degree of freedom of the data. We fitted GAMMs for all subjects and separately for male and female subjects. Using these GAMM fits, we generated spatial maps of cerebellocortical FC for children from birth to 60 months. We then applied spatial z-normalization and probabilistic threshold-free cluster enhancement (pTFCE)[122] to obtain enhanced p-value maps. We derived cerebellar functional parcellations at each time point using a winner-take-all strategy, labeling each cerebellar voxel according to the FC component with the lowest enhanced p-value. We specifically focused on the time points of 0, 3, 6, 9, 12, 18, 24, 36, 48, and 60 months to examine the developmental trajectory of cerebellocortical FC.

Functional Connectivity Trajectories The 99th percentile FC value of each cortical RSN with the entire cerebellum was used to display the functional connectivity developmental trends during early childhood.

Growth Rates Using the cerebellar functional parcellation map at 60 months, we computed the 99th percentile FC for each cortical RSN and calculated the percentage FC changes between two time points:

$$\frac{\text{FC at current time point} - \text{FC at previous time point}}{\text{FC at previous time point}} \times 100\%. \tag{1}$$

Volumetric Trajectories The volume fraction of each network was determined based on winner-take-all parcellation. Trajectories of cerebellar volume fractions were modeled using third-degree polynomial regression analysis with the `lm` function in R: $\texttt{poly}(\texttt{month}', \texttt{degree} = 3)$ with $\texttt{month}' = \log_2\left(\frac{\texttt{month}}{12} + 1\right)$. A logarithmic time scale better captures the rapid changes in the first year of life.

Laterality The laterality index (LI) was calculated as

$$\mathrm{LI} = \frac{\mathrm{L_{norm}} - \mathrm{R_{norm}}}{\mathrm{L_{norm}} + \mathrm{R_{norm}}}, \tag{2}$$

where L_{norm} and R_{norm} are the voxel counts in the left and right cerebellar hemispheres, normalized by the total voxel count in each respective hemisphere. LI ranges between -1 (total leftward lateralization) and 1 (total rightward lateralization) with 0 indicating complete symmetry.

Visualization Cortical functional networks were visualized using MRIcroGL (`https://www.nitrc.org/projects/mricrogl/`). Cerebellocortical FC flat maps were displayed using the Statistical Parametric Mapping software package (SPM12, `https://www.fil.ion.ucl.ac.uk/spm/software/spm12/`) and the SUIT[36] software package (`https://github.com/jdiedrichsen/suit`). Functional gradient maps were generated by LittleBrain[42]. Trajectories of cerebellocortical FC across age were analyzed and visualized using ggplot2[123] in R.

Supplementary Information The manuscript contains supplementary material.

Acknowledgements This work was supported in part by the United States National Institutes of Health (NIH) under grants R01 MH125479, R01 EB008374, and R01 MH133836.

Author Contributions W.L.: methodology, investigation, visualization, data curation, writing – original draft, writing — review and editing. K.-H.T.: data curation, methodology, software, visualization, writing — review and editing. K.M.H.: resources, writing — review and editing. L.W.: resources. W.L.: resources. S.A.: resources, writing — review and editing. P.-T.Y.: conceptualization, supervision, funding acquisition, investigation, validation, writing — review and editing.

Code Availability Software packages used in this work include FSL v.6.0.7.6, ICA-AROMA, ANTs, MATLAB (toolboxes include BrainNet Viewer, Network Community Toolbox, SPM12, SUIT, etc.), Python v.3.12, R v.3.8.0 (packages include gamm4, mgcv, bigmemory, ggplot2, etc.), and MRIcroGL.

Competing Interests The authors declare that they have no competing financial interests.

Correspondence Correspondence and requests for materials should be addressed to P.-T.Y.

1. Adamaszek, M. *et al.* Consensus paper: Cerebellum and emotion. *The Cerebellum* **16**, 552–576 (2017). URL http://link.springer.com/10.1007/s12311-016-0815-8.

2. Hayter, A., Langdon, D. & Ramnani, N. Cerebellar contributions to working memory. *NeuroImage* **36**, 943–954 (2007). URL https://linkinghub.elsevier.com/retrieve/pii/S1053811907001802.

3. Timmann, D. *et al.* The human cerebellum contributes to motor, emotional and cognitive associative learning. a review. *Cortex* **46**, 845–857 (2010). URL https://linkinghub.elsevier.com/retrieve/pii/S0010945209002044.

4. Diedrichsen, J., King, M., Hernandez-Castillo, C., Sereno, M. & Ivry, R. B. Universal transform or multiple functionality? understanding the contribution of the human cerebellum across task domains. *Neuron* **102**, 918–928 (2019). URL https://linkinghub.elsevier.com/retrieve/pii/S0896627319303782.

5. Barton, R. A. & Venditti, C. Rapid evolution of the cerebellum in humans and other great apes. *Current Biology* **24**, 2440–2444 (2014). URL https://www.sciencedirect.com/science/article/pii/S0960982214010690.

6. Smaers, J. B. & Vanier, D. R. Brain size expansion in primates and humans is explained by a selective modular expansion of the cortico-cerebellar system. *Cortex* **118**, 292–305 (2019). URL https://www.sciencedirect.com/science/article/pii/S0010945219301960.

7. Dellatolas, G. & Câmara-Costa, H. The role of cerebellum in the child neuropsychological functioning. In *Handbook of Clinical Neurology*, vol. 173, 265–304 (Elsevier, 2010). URL https://linkinghub.elsevier.com/retrieve/pii/B978044464150200023X.

8. Volpe, J. J. Cerebellum of the premature infant: Rapidly developing, vulnerable, clinically important. *Journal of Child Neurology* **24**, 1085–1104 (2009). URL http://journals.sagepub.com/doi/10.1177/0883073809338067.

9. Limperopoulos, C., Chilingaryan, G., Guizard, N., Robertson, R. L. & Du Plessis, A. J. Cerebellar injury in the premature infant is associated with impaired growth of specific cerebral regions. *Pediatric research* **68**, 145–150 (2010). URL https://www.nature.com/articles/pr2010148.

10. von Hofsten, C. & Rönnqvist, L. Preparation for grasping an object: a developmental study. *Journal of experimental psychology: Human perception and performance* **14**, 610 (1988). URL https://doi.org/10.1037/0096-1523.14.4.610.

11. Butterworth, G., Verweij, E. & Hopkins, B. The development of prehension in infants: Halverson revisited. *British Journal of Developmental Psychology* **15**, 223–236 (1997). URL https://doi.org/10.1111/j.2044-835X.1997.tb00736.x.

12. Karasik, L. B., Tamis-LeMonda, C. S. & Adolph, K. E. Transition from crawling to walking and infants' actions with objects and people. *Child Development* **82**, 1199–1209 (2011). URL https://srcd.onlinelibrary.wiley.com/doi/full/10.1111/j.1467-8624.2011.01595.x.

13. Adolph, K. E., Berger, S. E. & Leo, A. J. Developmental continuity? crawling, cruising, and walking. *Developmental Science* **14**, 306–318 (2011). URL https://onlinelibrary.wiley.com/doi/full/10.1111/j.1467-7687.2010.00981.x.

14. Malina, R. M. Motor development during infancy and early childhood: Overview and suggested directions for research. *International Journal of Sport and Health Science* **2**, 50–66 (2004). URL https://doi.org/10.5432/ijshs.2.50.

15. Gerber, R. J., Wilks, T. & Erdie-Lalena, C. Developmental milestones: motor development. *Pediatrics in Review* **31**, 267–277 (2010). URL https://doi.org/10.1542/pir.31-7-267.

16. Tomasello, M. Language development. *The Wiley-Blackwell handbook of childhood cognitive development* 239–257 (2011). URL https://onlinelibrary.wiley.com/doi/pdf/10.1002/9781444325485#page=249.

17. Gilmore, J. H., Knickmeyer, R. C. & Gao, W. Imaging structural and functional brain development in early childhood. *Nature Reviews Neuroscience* **19**, 123–137 (2018). URL https://www.nature.com/articles/nrn.2018.1.

18. Strüber, N. & Roth, G. *Developmental Neurobiology, In: Psychoneuroscience*, 117–141 (Springer Berlin Heidelberg, Berlin, Heidelberg, 2023). URL https://doi.org/10.1007/978-3-662-65774-4_5.

19. O'Reilly, J. X., Beckmann, C. F., Tomassini, V., Ramnani, N. & Johansen-Berg, H. Distinct and overlapping functional zones in the cerebellum defined by resting state functional connectivity. *Cerebral Cortex* **20**, 953–965 (2010). URL https://doi.org/10.1093/cercor/bhp157.

20. Yeo, B. T. *et al.* The organization of the human cerebral cortex estimated by intrinsic functional connectivity. *Journal of neurophysiology* (2011). URL https://doi.org/10.1152/jn.00338.2011.

21. Sang, L. *et al.* Resting-state functional connectivity of the vermal and hemispheric subregions of the cerebellum with both the cerebral cortical networks and subcortical structures. *NeuroImage* **61**, 1213–1225 (2012). URL https://linkinghub.elsevier.com/retrieve/pii/S1053811912003928.

22. Habas, C. *et al.* Distinct Cerebellar Contributions to Intrinsic Connectivity Networks. *Journal of Neuroscience* **29**, 8586–8594 (2009). URL https://www.jneurosci.org/content/29/26/8586.

23. Guell, X., Gabrieli, J. D. & Schmahmann, J. D. Triple representation of language, working memory, social and emotion processing in the cerebellum: convergent evidence from task and seed-based resting-state fMRI analyses in a single large cohort. *NeuroImage* **172** (2018). URL https://linkinghub.elsevier.com/retrieve/pii/S105381191830082X.

24. Guell, X., Schmahmann, J. D., Gabrieli, J. D. & Ghosh, S. S. Functional gradients of the cerebellum. *eLife* **7**, e36652 (2018). URL https://elifesciences.org/articles/36652.

25. Guell, X. & Schmahmann, J. Cerebellar functional anatomy: a didactic summary based on human fmri evidence. *The Cerebellum* **19**, 1–5 (2020). URL https://link.springer.com/article/10.1007/s12311-019-01083-9.

26. Xue, A. *et al.* The detailed organization of the human cerebellum estimated by intrinsic functional connectivity within the individual. *Journal of neurophysiology* **125**, 358–384 (2021). URL https://journals.physiology.org/doi/full/10.1152/jn.00561.2020.

27. Kipping, J. A., Tuan, T. A., Fortier, M. V. & Qiu, A. Asynchronous development of cerebellar, cerebello-cortical, and cortico-cortical functional networks in infancy, childhood, and adulthood. *Cerebral Cortex* 5170–5184 (2016). URL http://cercor.oxfordjournals.org/cgi/doi/10.1093/cercor/bhw298.

28. Diamond, A. Close interrelation of motor development and cognitive development and of the cerebellum and prefrontal cortex. *Child Development* **71**, 44–56 (2000). URL https://srcd.onlinelibrary.wiley.com/doi/abs/10.1111/1467-8624.00117. https://srcd.onlinelibrary.wiley.com/doi/pdf/10.1111/1467-8624.00117.

29. Konrad, K. & Eickhoff, S. B. Is the ADHD brain wired differently? A review on structural and functional connectivity in attention deficit hyperactivity disorder. *Human Brain Mapping* **31**, 904–916 (2010). URL https://onlinelibrary.wiley.com/doi/full/10.1002/hbm.21058.

30. Rubia, K. Cognitive neuroscience of attention deficit hyperactivity disorder (ADHD) and its clinical translation. *Frontiers in Human Neuroscience* **12**, 100 (2018). URL http://journal.frontiersin.org/article/10.3389/fnhum.2018.00100/full.

31. Verly, M. *et al.* Altered functional connectivity of the language network in ASD: Role of classical language areas and cerebellum. *NeuroImage: Clinical* **4**, 374–382 (2014). URL https://www.sciencedirect.com/science/article/pii/S2213158214000096.

32. Khan, A. J. *et al.* Cerebro-cerebellar resting-state functional connectivity in children and adolescents with autism spectrum disorder. *Biological Psychiatry* **78**, 625–634 (2015). URL https://www.sciencedirect.com/science/article/pii/S0006322315002735.

33. Ramos, T. C., Balardin, J. B., Sato, J. R. & Fujita, A. Abnormal cortico-cerebellar functional connectivity in autism spectrum disorder. *Frontiers in Systems Neuroscience* **12** (2019). URL https://www.frontiersin.org/articles/10.3389/fnsys.2018.00074.

34. Adamaszek, M., Manto, M. & Schutter, D. J. L. G. (eds.) *The Emotional Cerebellum*, vol. 1378 of *Advances in Experimental Medicine and Biology* (Springer International Publishing, 2022). URL https://link.springer.com/10.1007/978-3-030-99550-8.

35. Howell, B. R. *et al.* The UNC/UMN baby connectome project (BCP): An overview of the study design and protocol development. *NeuroImage* **185**, 891–905 (2019). URL https://linkinghub.elsevier.com/retrieve/pii/S1053811918302593.

36. Diedrichsen, J. A spatially unbiased atlas template of the human cerebellum. *NeuroImage* **33**, 127–38 (2006). URL https://www.ncbi.nlm.nih.gov/pubmed/16904911.

37. Schmahmann, J. D. *et al.* Three-dimensional mri atlas of the human cerebellum in proportional stereotaxic space. *Neuroimage* **10**, 233–260 (1999). URL https://www.ncbi.nlm.nih.gov/pubmed/10458940.

38. Diedrichsen, J. & Zotow, E. Surface-based display of volume-averaged cerebellar imaging data. *PLOS ONE* **10**, e0133402 (2015). URL https://dx.plos.org/10.1371/journal.pone.0133402.

39. van Es, D. M., van der Zwaag, W. & Knapen, T. Topographic maps of visual space in the human cerebellum. *Current Biology* **29**, 1689–1694 (2019). URL https://doi.org/10.1016/j.cub.2019.04.012.

40. Buckner, R. L., Krienen, F. M., Castellanos, A., Diaz, J. C. & Yeo, B. T. T. The organization of the human cerebellum estimated by intrinsic functional connectivity. *Journal of Neurophysiology* **106**, 2322–2345 (2011). URL https://journals.physiology.org/doi/full/10.1152/jn.00339.2011. Publisher: American Physiological Society.

41. King, M., Hernandez-Castillo, C. R., Poldrack, R. A., Ivry, R. B. & Diedrichsen, J. Functional boundaries in the human cerebellum revealed by a multi-domain task battery. *Nature Neuroscience* **22**, 1371–1378 (2019). URL https://www.nature.com/articles/s41593-019-0436-x.

42. Guell, X. *et al.* LittleBrain: A gradient-based tool for the topographical interpretation of cerebellar neuroimaging findings. *PLOS ONE* **14**, e0210028 (2019). URL https://journals.plos.org/plosone/article?id=10.1371/journal.pone.0210028.

43. Zhang, D. *et al.* Intrinsic functional relations between human cerebral cortex and thalamus. *Journal of Neurophysiology* **100**, 1740–1748 (2008). URL https://www.physiology.org/doi/10.1152/jn.90463.2008.

44. Greene, D. J. *et al.* Developmental changes in the organization of functional connections between the basal ganglia and cerebral cortex. *Journal of Neuroscience* **34**, 5842–5854 (2014).

45. Wang, S. S.-H., Kloth, A. D. & Badura, A. The Cerebellum, Sensitive Periods, and Autism. *Neuron* **83**, 518–532 (2014). URL https://www.cell.com/neuron/abstract/S0896-6273(14)00627-8.

46. Menon, V. & Uddin, L. Q. Saliency, switching, attention and control: a network model of insula function. *Brain Structure and Function* **214**, 655–667 (2010). URL https://doi.org/10.1007/s00429-010-0262-0.

47. Menon, V., Palaniyappan, L. & Supekar, K. Integrative brain network and salience models of psychopathology and cognitive dysfunction in schizophrenia. *Biological Psychiatry* **94**, 108–120 (2023). URL https://linkinghub.elsevier.com/retrieve/pii/S0006322322016377.

48. Hu, D., Shen, H. & Zhou, Z. Functional asymmetry in the cerebellum: a brief review. *The Cerebellum* **7**, 304–313 (2008). URL https://link.springer.com/article/10.1007/s12311-008-0031-2.

49. E, K., Chen, S. A., Ho, M. R. & Desmond, J. E. A meta-analysis of cerebellar contributions to higher cognition from PET and fMRI studies. *Human Brain Mapping* **35** (2012). URL https://www.ncbi.nlm.nih.gov/pmc/articles/PMC3866223/.

50. Marek, S. *et al.* Spatial and temporal organization of the individual human cerebellum. *Neuron* **100**, 977–993.e7 (2018). URL https://linkinghub.elsevier.com/retrieve/pii/S0896627318308985.

51. Chechik, G., Meilijson, I. & Ruppin, E. Synaptic Pruning in Development: A Computational Account. *Neural Computation* **10**, 1759–1777 (1998). URL https://direct.mit.edu/neco/article/10/7/1759-1777/6200.

52. Wiestler, T., McGonigle, D. J. & Diedrichsen, J. Integration of sensory and motor representations of single fingers in the human cerebellum. *Journal of Neurophysiology* **105**, 3042–3053 (2011). URL https://journals.physiology.org/doi/full/10.1152/jn.00106.2011.

53. Paulin, M. G. The role of the cerebellum in motor control and perception. *Brain Behavior and Evolution* **41**, 39–50 (1993). URL https://doi.org/10.1159/000113822.

54. Glickstein, M. What does the cerebellum really do? *Current Biology* **17**, R824–R827 (2007). URL https://doi.org/10.1016/j.cub.2007.08.009.

55. Sasaki, K. Cerebro-cerebellar interactions and organization of a fast and stable hand movement: Cerebellar participation in voluntary movement and motor learning. In *Cerebellar Functions*, 70–85 (Springer, 1985).

56. Nawrot, M. & Rizzo, M. Motion perception deficits from midline cerebellar lesions in human. *Vision Research* **35**, 723–731 (1995). URL https://linkinghub.elsevier.com/retrieve/pii/004269899400168L.

57. Wheelock, M. D. *et al.* Altered functional network connectivity relates to motor development in children born very preterm. *NeuroImage* **183**, 574–583 (2018). URL https://www.sciencedirect.com/science/article/pii/S1053811918307493.

58. Ren, J. *et al.* Dissociable auditory cortico-cerebellar pathways in the human brain estimated by intrinsic functional connectivity. *Cerebral Cortex* **31**, 2898–2912 (2021). URL https://academic.oup.com/cercor/article/31/6/2898/6120329.

59. Fransson, P., Åden, U., Blennow, M. & Lagercrantz, H. The functional architecture of the infant brain as revealed by resting-state fMRI. *Cerebral Cortex* **21**, 145–154 (2010). URL https://doi.org/10.1093/cercor/bhq071. https://academic.oup.com/cercor/article-pdf/21/1/145/17304017/bhq071.pdf.

60. Pieterman, K. *et al.* Cerebello-cerebral connectivity in the developing brain. *Brain Structure and Function* **222**, 1625–1634 (2017).

61. Dijkshoorn, A. B. *et al.* Preterm infants with isolated cerebellar hemorrhage show bilateral cortical alterations at term equivalent age. *Scientific Reports* **10**, 5283 (2020). URL https://www.nature.com/articles/s41598-020-62078-9.

62. Brossard-Racine, M., Du Plessis, A. J. & Limperopoulos, C. Developmental cerebellar cognitive affective syndrome in ex-preterm survivors following cerebellar injury. *The Cerebellum* **14**, 151–164 (2015). URL https://link.springer.com/article/10.1007/s12311-014-0597-9.

63. Hortensius, L. M. *et al.* Neurodevelopmental consequences of preterm isolated cerebellar hemorrhage: A systematic review. *Pediatrics* **142** (2018). URL https://publications.aap.org/pediatrics/article/142/5/e20180609/38536/Neurodevelopmental-Consequences-of-Preterm.

64. Raz, G. & Saxe, R. Learning in infancy is active, endogenously motivated, and depends on the prefrontal cortices. *Annual Review of Developmental Psychology* **2**, 247–268 (2020). URL https://doi.org/10.1146/annurev-devpsych-121318-084841.

65. Lyu, W., Wu, Y., Huynh, K. M., Ahmad, S. & Yap, P.-T. A multimodal submillimeter MRI atlas of the human cerebellum. *Scientific Reports* **14**, 5622 (2024).

66. Okayasu, M. *et al.* The Stroop effect involves an excitatory–inhibitory fronto-cerebellar loop. *Nature Communications* **14**, 27 (2023). URL https://www.nature.com/articles/s41467-022-35397-w.

67. Margulies, D. S. *et al.* Situating the default-mode network along a principal gradient of macroscale cortical organization. *Proceedings of the National Academy of Sciences* **113**, 12574–12579 (2016).

68. Sydnor, V. J. *et al.* Neurodevelopment of the association cortices: Patterns, mechanisms, and implications for psychopathology. *Neuron* **109**, 2820–2846 (2021). URL https://linkinghub.elsevier.com/retrieve/pii/S0896627321004578.

69. Keller, A. S. *et al.* Personalized functional brain network topography is associated with individual differences in youth cognition. *Nature Communications* **14**, 8411 (2023). URL https://www.nature.com/articles/s41467-023-44087-0.

70. Luo, A. C. *et al.* Functional connectivity development along the sensorimotor-association axis enhances the cortical hierarchy. *Nature Communications* **15** (2024). URL https://www.nature.com/articles/s41467-024-47748-w.

71. Wang, Y. *et al.* Spatio-molecular profiles shape the human cerebellar hierarchy along the sensorimotor-association axis. *Cell Reports* **43**, 113770 (2024). URL https://linkinghub.elsevier.com/retrieve/pii/S2211124724000986.

72. Margulies, D. S. *et al.* Situating the default-mode network along a principal gradient of macroscale cortical organization. *Proceedings of the National Academy of Sciences* **113**, 12574–12579 (2016). URL https://www.pnas.org/doi/full/10.1073/pnas.1608282113.

73. Huntenburg, J. M., Bazin, P.-L. & Margulies, D. S. Large-Scale Gradients in Human Cortical Organization. *Trends in Cognitive Sciences* **22**, 21–31 (2018). URL https://www.cell.com/trends/cognitive-sciences/abstract/S1364-6613(17)30240-1.

74. Xia, Y. *et al.* Development of functional connectome gradients during childhood and adolescence. *Science Bulletin* **67**, 1049–1061 (2022). URL https://www.sciencedirect.com/science/article/pii/S2095927322000020.

75. Taylor, H. P. *et al.* Functional Hierarchy of the Human Neocortex from Cradle to Grave (2024). URL https://www.biorxiv.org/content/10.1101/2024.06.14.599109v1.

76. Ahmad, S. *et al.* Multifaceted atlases of the human brain in its infancy. *Nature Methods* **20**, 55–64 (2023). URL https://doi.org/10.1038/s41592-022-01703-z.

77. Knickmeyer, R. C. *et al.* A structural MRI study of human brain development from birth to 2 years. *The Journal of Neuroscience* **28**, 12176–12182 (2008). URL https://www.jneurosci.org/lookup/doi/10.1523/JNEUROSCI.3479-08.2008.

78. Yu, X. *et al.* Functional connectivity in infancy and toddlerhood predicts long-term language and preliteracy outcomes. *Cerebral Cortex* **32**, 725–736 (2022). URL https://academic.oup.com/cercor/article/32/4/725/6339270.

79. Magnuson, K. A., Ruhm, C. & Waldfogel, J. Does prekindergarten improve school preparation and performance? *Economics of Education review* **26**, 33–51 (2007). URL https://www.sciencedirect.com/science/article/pii/S0272775706000434.

80. Weiland, C. & Yoshikawa, H. Impacts of a prekindergarten program on children's mathematics, language, literacy, executive function, and emotional skills. *Child Development* **84**, 2112–2130 (2013). URL https://srcd.onlinelibrary.wiley.com/doi/full/10.1111/cdev.12099.

81. Kolk, S. M. & Rakic, P. Development of prefrontal cortex. *Neuropsychopharmacology* **47**, 41–57 (2022).

82. Friedman, N. P. & Robbins, T. W. The role of prefrontal cortex in cognitive control and executive function. *Neuropsychopharmacology* **47**, 72–89 (2022).

83. Hodel, A. S. Rapid infant prefrontal cortex development and sensitivity to early environmental experience. *Developmental Review* **48**, 113–144 (2018). URL https://www.sciencedirect.com/science/article/pii/S0273229717300825.

84. Hendry, A., Jones, E. J. & Charman, T. Executive function in the first three years of life: Precursors, predictors and patterns. *Developmental Review* **42**, 1–33 (2016). URL https://www.sciencedirect.com/science/article/pii/S0273229716300363.

85. Dehaene-Lambertz, G., Dehaene, S. & Hertz-Pannier, L. Functional neuroimaging of speech perception in infants. *Science* **298**, 2013–2015 (2002). URL https://www.science.org/doi/full/10.1126/science.1077066.

86. Middleton, F. A. & Strick, P. L. Cerebellar projections to the prefrontal cortex of the primate. *Journal of Neuroscience* **21**, 700–712 (2001). URL https://www.jneurosci.org/content/21/2/700.

87. Kelly, R. M. & Strick, P. L. Cerebellar loops with motor cortex and prefrontal cortex of a nonhuman primate. *Journal of Neuroscience* **23**, 8432–8444 (2003). URL https://www.jneurosci.org/content/23/23/8432.full.

88. Krienen, F. M. & Buckner, R. L. Segregated fronto-cerebellar circuits revealed by intrinsic functional connectivity. *Cerebral Cortex* **19**, 2485–2497 (2009). URL https://academic.oup.com/cercor/article-lookup/doi/10.1093/cercor/bhp135.

89. Scott, R. B. *et al.* Lateralized cognitive deficits in children following cerebellar lesions. *Developmental Medicine & Child Neurology* **43**, 685–691 (2001). URL https://doi.org/10.1111/j.1469-8749.2001.tb00142.x.

90. Starowicz-Filip, A. *et al.* Cerebellar functional lateralization from the perspective of clinical neuropsychology. *Frontiers in Psychology* **12**, 775308 (2021). URL https://www.frontiersin.org/journals/psychology/articles/10.3389/fpsyg.2021.775308/full.

91. Liu, H., Stufflebeam, S. M., Sepulcre, J., Hedden, T. & Buckner, R. L. Evidence from intrinsic activity that asymmetry of the human brain is controlled by multiple factors. *Proceedings of the National Academy of Sciences* **106**, 20499–20503 (2009). URL https://www.pnas.org/doi/full/10.1073/pnas.0908073106.

92. Güntürkün, O., Ströckens, F. & Ocklenburg, S. Brain Lateralization: A Comparative Perspective. *Physiological Reviews* **100**, 1019–1063 (2020). URL https://journals.physiology.org/doi/full/10.1152/physrev.00006.2019.

93. Pilgrim, C. & Reisert, I. Differences between male and female brains - developmental mechanisms and implications. *Hormone and Metabolic Research* **24**, 353–359 (1992). URL http://www.thieme-connect.de/DOI/DOI?10.1055/s-2007-1003334.

94. Zaidi, Z. F. Gender differences in human brain: A review. *The Open Anatomy Journal* **2**, 37–55 (2010). URL http://benthamopen.com/ABSTRACT/TOANATJ-2-37.

95. Camarata, S. & Woodcock, R. Sex differences in processing speed: Developmental effects in males and females. *Intelligence* **34**, 231–252 (2006).

96. Rhodes, M. E. & Rubin, R. T. Functional sex differences ('sexual diergism') of central nervous system cholinergic systems, vasopressin, and hypothalamic–pituitary–adrenal axis activity in mammals: A selective review. *Brain Research Reviews* (1999).

97. Fan, L. *et al.* Sexual dimorphism and asymmetry in human cerebellum: An MRI-based morphometric study. *Brain Research* **1353**, 60–73 (2010). URL https://www.sciencedirect.com/science/article/pii/S0006899310015933.

98. Tiemeier, H. *et al.* Cerebellum development during childhood and adolescence: A longitudinal morphometric MRI study. *NeuroImage* **49**, 63–70 (2010). URL https://linkinghub.elsevier.com/retrieve/pii/S1053811909008933.

99. Wang, Y. *et al.* Longitudinal development of the cerebellum in human infants during the first 800 days. *Cell Reports* **42**, 112281 (2023). URL https://linkinghub.elsevier.com/retrieve/pii/S2211124723002929.

100. Zahn-Waxler, C., Crick, N. R., Shirtcliff, E. A. & Woods, K. E. The origins and development of psychopathology in females and males. In *Developmental Psychopathology*, 76–138 (John Wiley & Sons, Ltd, 2015). URL https://onlinelibrary.wiley.com/doi/abs/10.1002/9780470939383.ch4.

101. Verly, M. *et al.* Altered functional connectivity of the language network in ASD: role of classical language areas and cerebellum. *NeuroImage: Clinical* **4**, 374–382 (2014).

102. Kucyi, A., Hove, M. J., Biederman, J., Van Dijk, K. R. & Valera, E. M. Disrupted functional connectivity of cerebellar default network areas in attention-deficit/hyperactivity disorder. *Human Brain Mapping* **36**, 3373–3386 (2015).

103. Özçalışkan, Ş. & Goldin-Meadow, S. Sex differences in language first appear in gesture. *Developmental science* **13**, 752–760 (2010).

104. Tse, S. K., Chan, C., Li, H. & Kwong, S. M. Sex differences in syntactic development: Evidence from cantonese-speaking preschoolers in hong kong. *International Journal of Behavioral Development* **26**, 509–517 (2002).

105. Zhang, H., Shen, D. & Lin, W. Resting-state functional MRI studies on infant brains: A decade of gap-filling efforts. *NeuroImage* **185**, 664–684 (2019). URL https://linkinghub.elsevier.com/retrieve/pii/S1053811918305962.

106. Jenkinson, M., Bannister, P., Brady, M. & Smith, S. Improved optimization for the robust and accurate linear registration and motion correction of brain images. *NeuroImage* **17**, 825–841 (2002). URL https://www.sciencedirect.com/science/article/pii/S1053811902911328.

107. Andersson, J. L., Skare, S. & Ashburner, J. How to correct susceptibility distortions in spin-echo echo-planar images: application to diffusion tensor imaging. *NeuroImage* **20**, 870–888 (2003). URL https://www.sciencedirect.com/science/article/pii/S1053811903003367.

108. Smith, S. M. *et al.* Advances in functional and structural MR image analysis and implementation as FSL. *NeuroImage* **23**, S208–S219 (2004). URL https://www.sciencedirect.com/science/article/pii/S1053811904003933.

109. Greve, D. N. & Fischl, B. Accurate and robust brain image alignment using boundary-based registration. *NeuroImage* **48**, 63–72 (2009). URL https://doi.org/10.1016/j.neuroimage.2009.06.060.

110. Glasser, M. F. *et al.* A multi-modal parcellation of human cerebral cortex. *Nature* **536**, 171–178 (2016). URL https://www.nature.com/articles/nature18933.

111. Pruim, R. H. *et al.* ICA-AROMA: A robust ICA-based strategy for removing motion artifacts from fMRI data. *NeuroImage* **112**, 267–277 (2015).

112. Parkes, L., Fulcher, B., Yücel, M. & Fornito, A. An evaluation of the efficacy, reliability, and sensitivity of motion correction strategies for resting-state functional MRI. *NeuroImage* **171**, 415–436 (2018).

113. Power, J. D., Barnes, K. A., Snyder, A. Z., Schlaggar, B. L. & Petersen, S. E. Spurious but systematic correlations in functional connectivity MRI networks arise from subject motion. *NeuroImage* **59**, 2142–2154 (2012).

114. Jenkinson, M., Bannister, P., Brady, M. & Smith, S. Improved optimization for the robust and accurate linear registration and motion correction of brain images. *NeuroImage* **17**, 825–841 (2002).

115. Smith, S. M. *et al.* Correspondence of the brain's functional architecture during activation and rest. *Proceedings of the National Academy of Sciences* **106**, 13040–13045 (2009). URL `http://www.pnas.org/cgi/doi/10.1073/pnas.0905267106`.

116. Beckmann, C., Mackay, C., Filippini, N. & Smith, S. Group comparison of resting-state FMRI data using multi-subject ICA and dual regression. *NeuroImage* **47**, S148 (2009). URL `https://linkinghub.elsevier.com/retrieve/pii/S1053811909715113`.

117. Greicius, M. D., Krasnow, B., Reiss, A. L. & Menon, V. Functional connectivity in the resting brain: a network analysis of the default mode hypothesis. *Proceedings of the National Academy of Sciences* **100**, 253–258 (2003).

118. Yuen, N. H., Osachoff, N. & Chen, J. J. Intrinsic frequencies of the resting-state fMRI signal: the frequency dependence of functional connectivity and the effect of mode mixing. *Frontiers in Neuroscience* **13**, 463704 (2019).

119. Diedrichsen, J., Balsters, J. H., Flavell, J., Cussans, E. & Ramnani, N. A probabilistic MR atlas of the human cerebellum. *NeuroImage* **46**, 39–46 (2009).

120. Bro, R., Acar, E. & Kolda, T. G. Resolving the sign ambiguity in the singular value decomposition. *Journal of Chemometrics: A Journal of the Chemometrics Society* **22**, 135–140 (2008).

121. Wood, S. & Scheipl, F. *gamm4: Generalized additive mixed models using 'mgcv' and 'lme4'* (2017). URL `https://CRAN.R-project.org/package=gamm4`. R package version 0.2-6.

122. Spisák, T. *et al.* Probabilistic TFCE: A generalized combination of cluster size and voxel intensity to increase statistical power. *NeuroImage* **185**, 12–26 (2019).

123. Wickham, H. *ggplot2: Elegant Graphics for Data Analysis* (Springer-Verlag New York, 2016). URL `https://ggplot2.tidyverse.org`.

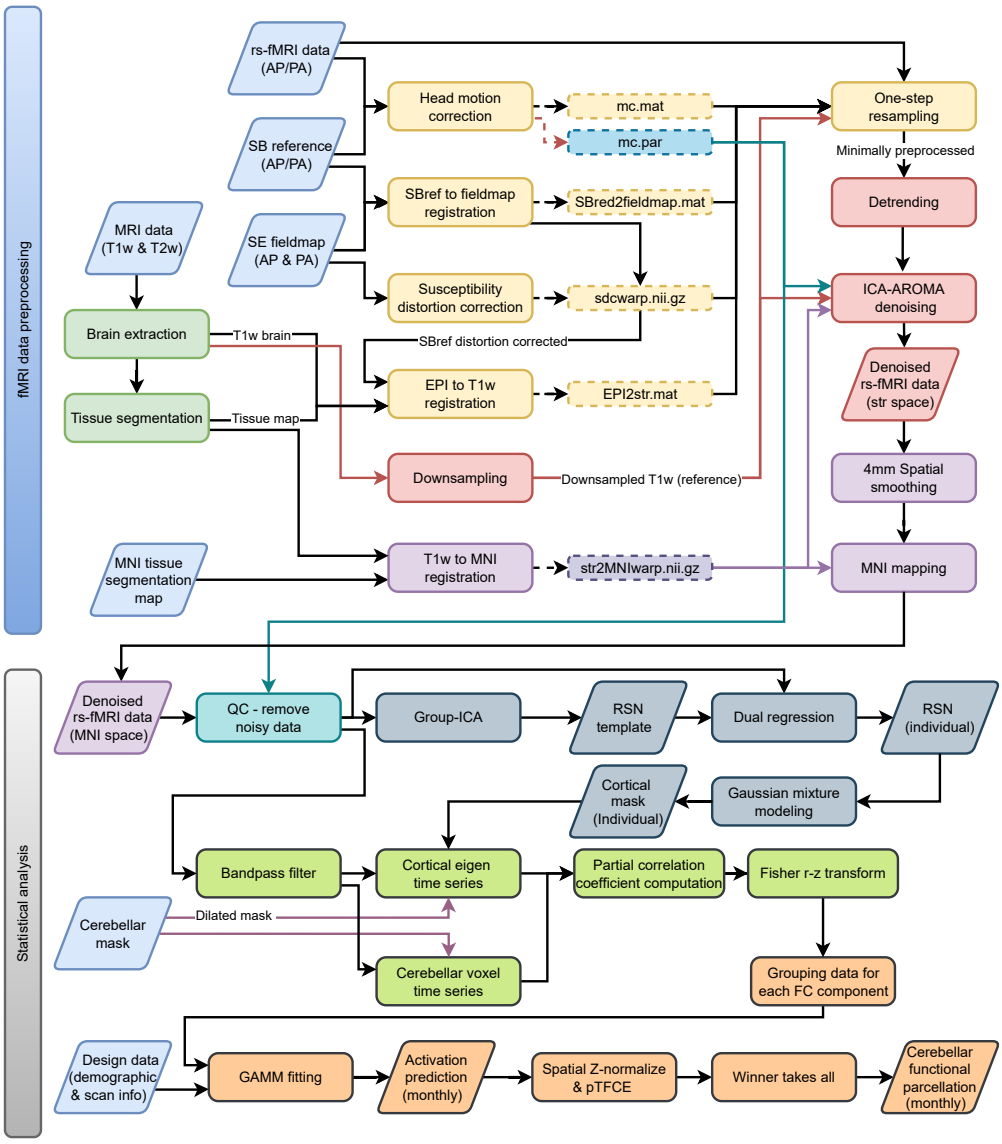

Fig. S1 | Data processing flowchart.

Tab. S1 | Cortical networks and their corresponding primary regions.

Network	Abbreviation	Primary Regions
Sensorimotor Network (SMN)		
Foot	SM-Foot	Bilateral precentral and postcentral gyri
Left hand	SM-Hand-L	Left precentral and postcentral gyri
Right hand	SM-Hand-R	Right precentral and postcentral gyri
Tongue	SM-Tongue	Bilateral precentral and postcentral gyri
Auditory Network (AUD)		
Auditory	AUD	Bilateral superior temporal gyri
Visual Network (VIS)		
Medial occipital	VIS-Occ-Med	Bilateral cuneus and lingual gyri
Lateral occipital	VIS-Lat	Bilateral cuneus, lingual gyri, and fusiform gyri
Superior occipital	VIS-Occ-Sup	Bilateral cuneus
Inferior occipital	VIS-Occ-Inf	Bilateral cuneus and lingual gyri
Occipital pole	VIS-Occ-Pol	Bilateral occipital poles
Salience Network (SN)		
Medial	SAL-Med	Anterior cingulate cortex and bilateral insulae
Lateral	SAL-Lat	Bilateral inferior frontal gyri and insulae
Ventral Attention Network (VAN)		
Frontal	VA-Front	Bilateral superior, middle, and inferior frontal gyri
Parietal	VA-Par	Bilateral paracentral lobes, supramarginal gyri, and insulae
Default Mode Network (DMN)		
Prefrontal	DM-Pref	Prefrontal cortex
Posterior cingulate	DM-Cing-Post	Posterior cingulate cortex and precuneus
Parietal angular	DM-Ang	Bilateral angular and middle temporal gyri
Left temporal	DM-Temp-L	Left middle temporal gyrus and temporal pole
Right temporal	DM-Temp-R	Right middle temporal gyrus and temporal pole
Parahippocampal	DM-PHippo	Bilateral parahippocampal, fusiform, and angular gyri
Executive Control Network (ECN)		
Prefrontal	EC-Pref	Prefrontal cortex
Left frontal	EC-Front-L	Left superior and middle frontal gyri
Right frontal	EC-Front-R	Right superior and middle frontal gyri
Supramarginal	EC-SMarg	Bilateral supramarginal gyri
Temporal	EC-Temp	Bilateral fusiform and inferior temporal gyri
Dorsal Attention Network (DAN)		
Medial parietal	DA-Par-Med	Bilateral precuneus and prefrontal cortices
Left parietal	DA-Par-L	Left superior parietal lobule
Right parietal	DA-Par-R	Right superior parietal lobule
Supramarginal	DA-SMarg	Bilateral supramarginal and inferior frontal gyri
Temporal	DA-Temp	Bilateral angular and inferior temporal gyri

Tab. S2 | Changes in 99th percentile cerebellocortical connectivity (%).

Network	0–3M	3–6M	6–9M	9–12M	12–18M	18–24M	0–12M	12–24M	24–36M	36–48M	48–60M
SM-Foot	-1.29	0.00	1.54	0.27	-0.51	-0.28	0.51	-0.78	-1.01	0.00	0.28
SM-Hand-L	-1.56	0.19	0.99	0.83	0.43	2.26	0.44	2.70	5.79	13.77	16.89
SM-Hand-R	-6.09	-0.97	-0.16	0.14	1.21	1.24	-7.02	2.46	2.67	6.87	9.16
SM-Tongue	1.08	5.13	3.23	1.04	8.68	-1.30	10.84	7.27	13.57	40.45	38.29
AUD	-35.07	-29.85	-21.99	-4.41	0.00	0.00	-66.03	0.00	13.94	29.59	23.52
VIS-Occ-Med	-0.14	3.93	5.42	4.82	5.02	3.52	14.68	8.72	4.80	5.35	6.31
VIS-Lat	2.90	4.00	3.11	2.83	7.37	5.88	13.47	13.69	2.76	-1.34	-0.44
VIS-Occ-Sup	-5.24	-1.93	-0.22	-0.77	-8.27	-5.55	-7.98	-13.36	-2.11	0.00	4.65
VIS-Occ-Inf	2.13	2.71	4.68	3.31	4.94	5.15	13.45	10.35	6.48	4.05	5.99
VIS-Occ-Pol	5.70	3.70	4.85	8.09	9.50	3.25	24.23	13.05	-3.40	-4.12	-0.09
SAL-Med	0.01	0.00	0.71	1.64	6.65	3.90	2.37	10.81	9.21	10.33	11.27
SAL-Lat	**48.69**	**26.92**	17.89	15.98	**46.64**	**27.12**	**158.01**	**86.41**	32.22	25.13	17.54
VA-Front	-2.60	-1.15	0.07	0.00	5.49	10.82	-3.65	16.90	24.81	25.70	19.41
VA-Par	-15.70	-8.72	0.00	1.24	7.81	14.55	-22.10	23.50	**63.83**	**57.45**	48.28
DM-Pref	-21.21	-11.54	-2.95	-1.49	0.58	0.01	-33.37	0.59	9.16	38.35	23.89
DM-Cing-Post	-11.49	-6.91	-3.79	-0.17	0.86	3.24	-20.86	4.13	19.41	28.51	12.77
DM-Ang	-2.83	-6.40	3.07	3.11	-4.42	4.79	-3.34	0.16	39.00	**63.99**	45.62
DM-Temp-L	-41.74	2.77	2.78	-0.65	16.79	**22.42**	-38.86	42.97	**87.64**	**83.40**	43.57
DM-Temp-R	-26.70	-10.40	-6.51	-4.85	-11.45	-8.80	-41.58	-19.25	37.02	**65.89**	43.36
DM-PHippo	3.60	11.35	7.96	5.89	4.47	-1.73	31.87	2.66	-8.49	-7.75	-4.66
EC-Pref	-3.46	7.06	5.27	14.06	15.05	13.44	24.11	30.51	25.63	27.62	41.04
EC-Front-L	-13.54	-4.85	-5.32	-0.52	0.60	0.73	-22.51	1.33	10.99	32.27	35.97
EC-Front-R	-13.24	-4.83	2.58	-0.27	4.46	9.49	-15.53	14.38	23.01	28.31	31.12
EC-SMarg	-47.25	-60.70	-40.46	-0.02	**21.00**	**33.92**	-87.66	**62.04**	**86.23**	**75.02**	**52.82**
EC-Temp	-5.09	-3.56	-4.31	-3.49	-3.49	-4.55	-15.48	-7.88	-3.99	-2.98	-0.41
DA-Par-Med	-19.36	-3.87	6.41	2.44	4.48	5.71	-15.49	10.44	4.35	25.48	32.19
DA-Par-L	-7.00	0.00	**38.23**	-6.77	15.74	**26.12**	19.85	45.97	**53.80**	43.33	32.10
DA-Par-R	-13.41	-13.71	-15.42	-16.95	-5.80	-1.72	-47.52	-7.42	-0.70	3.11	16.68
DA-SMarg	-15.95	-4.86	-2.18	1.22	**43.67**	**36.73**	-20.81	**96.44**	**61.22**	**53.78**	34.22
DA-Temp	1.99	7.89	3.15	0.53	0.46	0.49	14.10	0.95	-3.00	-6.70	-1.93

Note: Increases exceeding 20% within one year and annual increases exceeding 50% are shown in bold.

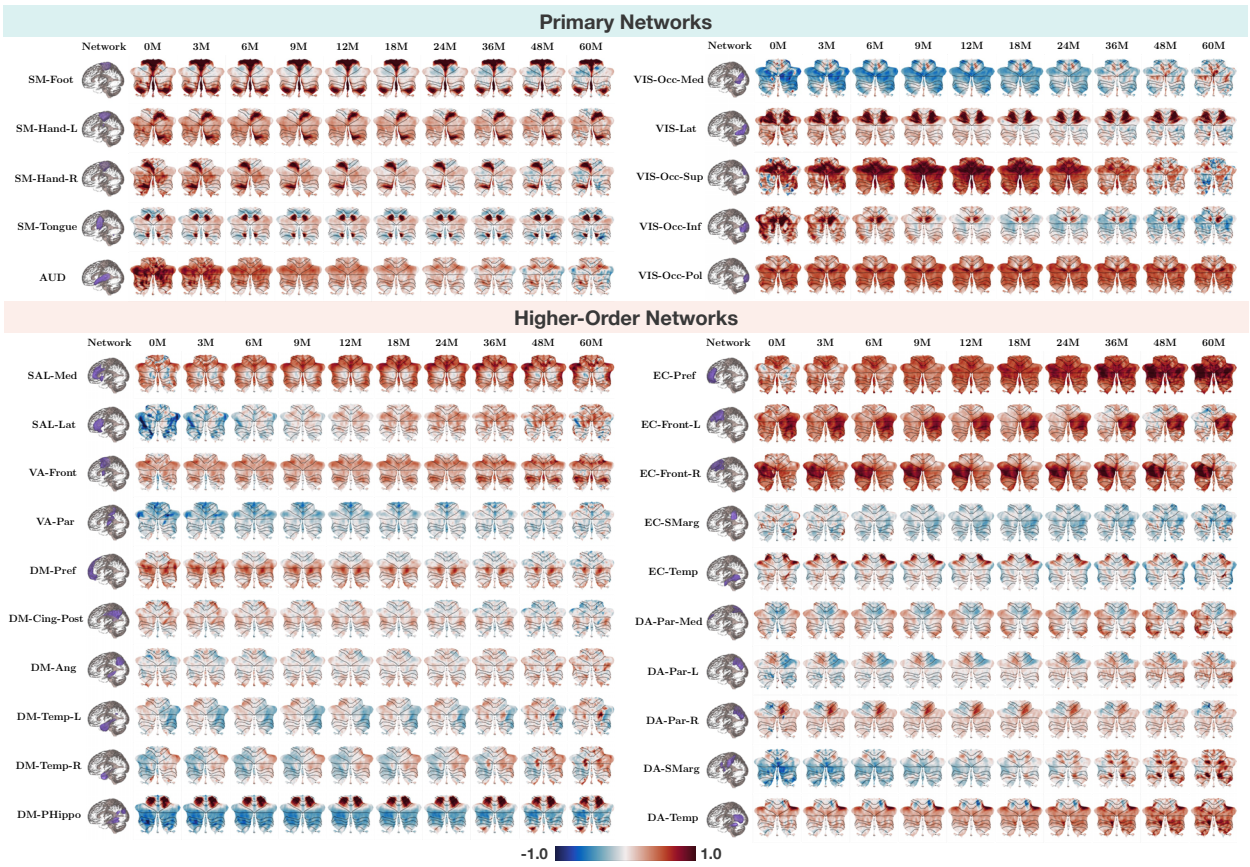

Fig. S2 | Cerebellar functional maps from birth to 60 months for children of both sexes. Spatiotemporal patterns of cerebellocortical connectivity (z-transformed) between the cerebellum and each RSN across early childhood. Values beyond −1.0 to 1.0 are capped for clarity.

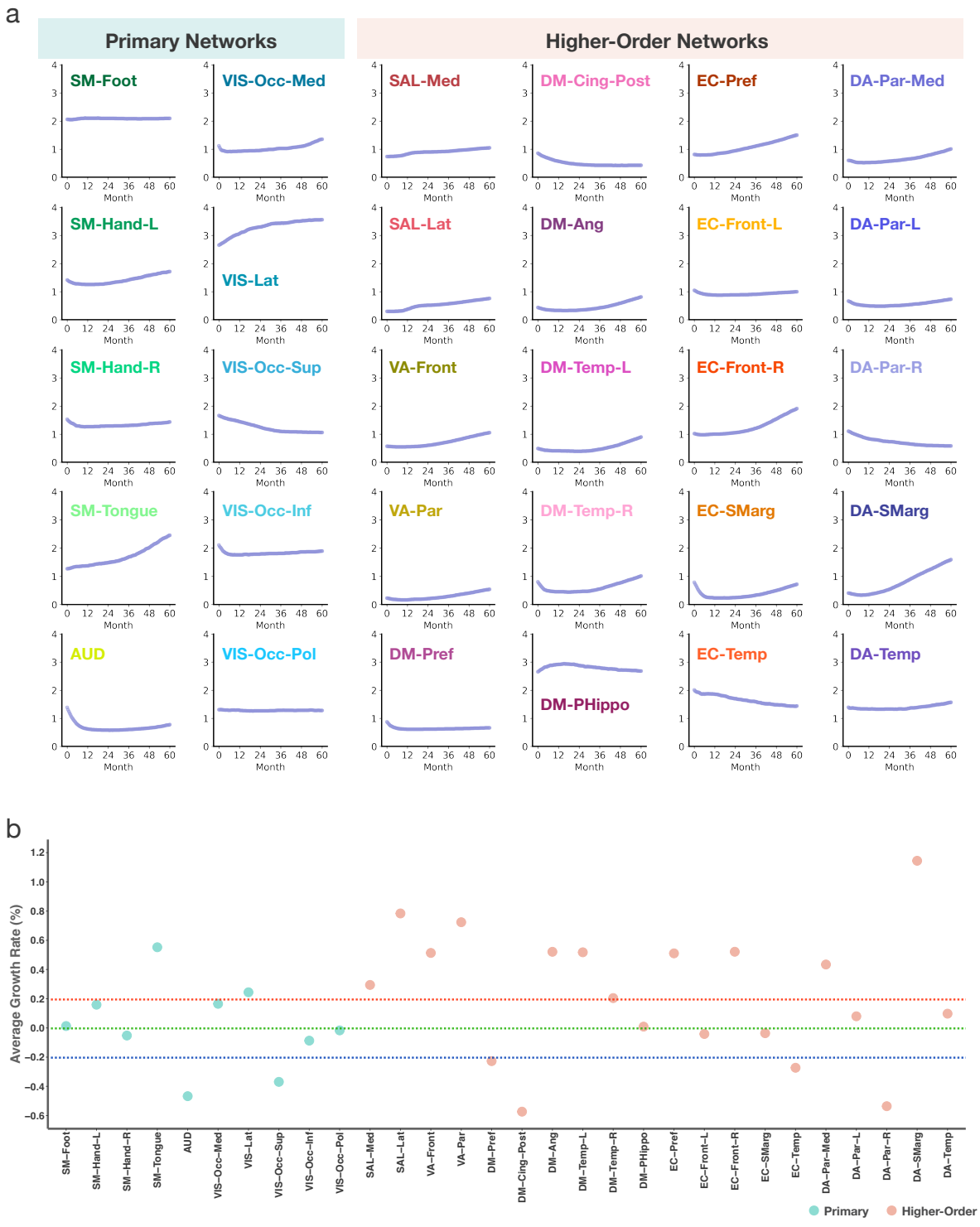

Fig. S3 | Developmental trends of cerebellocerebral connectivity. **a**, Trajectories of the 99th percentile cerebellar connectivity (z-transformed) with each RSN over time. **b**, Average biweekly growth rate of cerebellar connectivity with each RSN. Values above the red dashed line denote substantial positive growth, values around the green dashed line denote negligible or minimal growth, and values below the blue dashed line denote substantial negative growth.

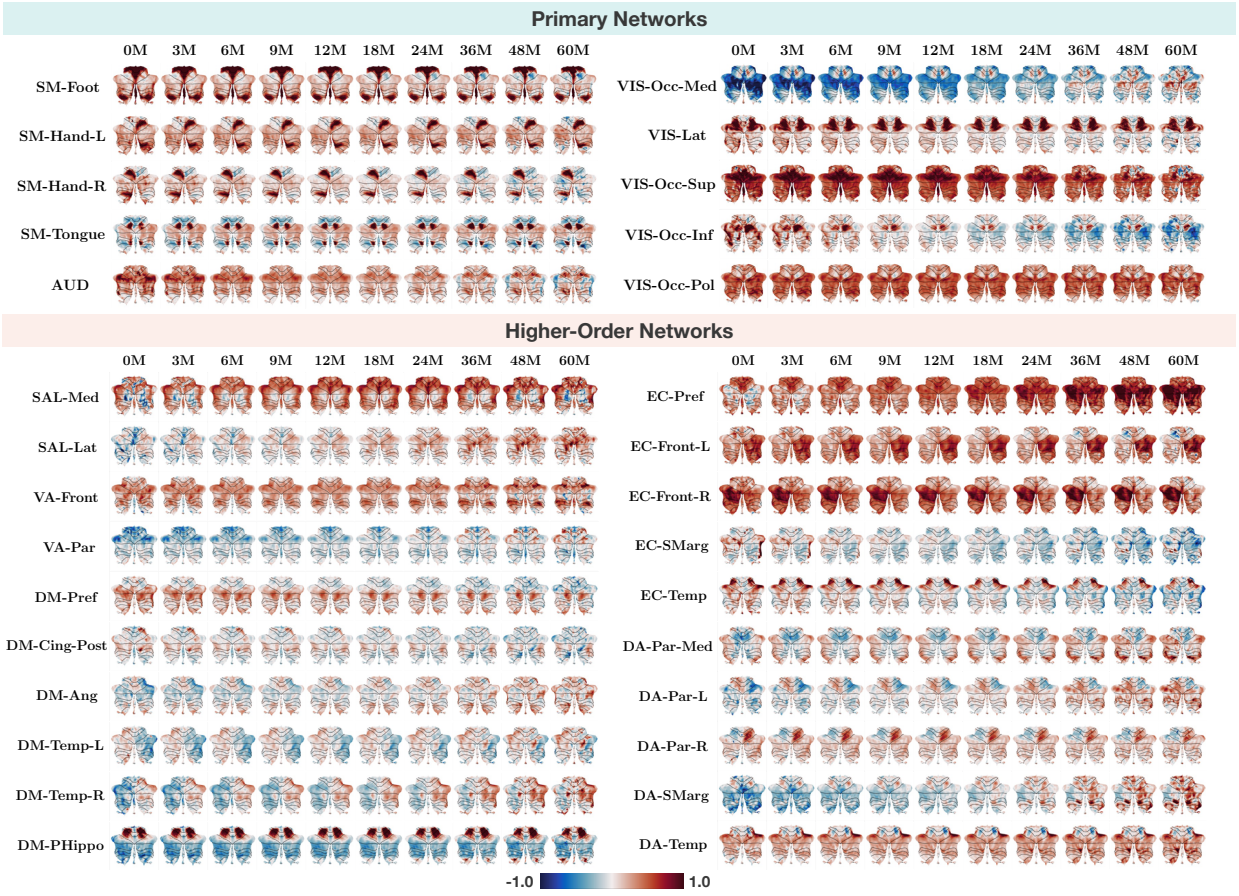

Fig. S4 | Cerebellar functional maps from birth to 60 months for female children. Spatiotemporal patterns of cerebellocortical connectivity (z-transformed) between the cerebellum and each RSN during early childhood in females. Values beyond −1.0 to 1.0 are capped for clarity.

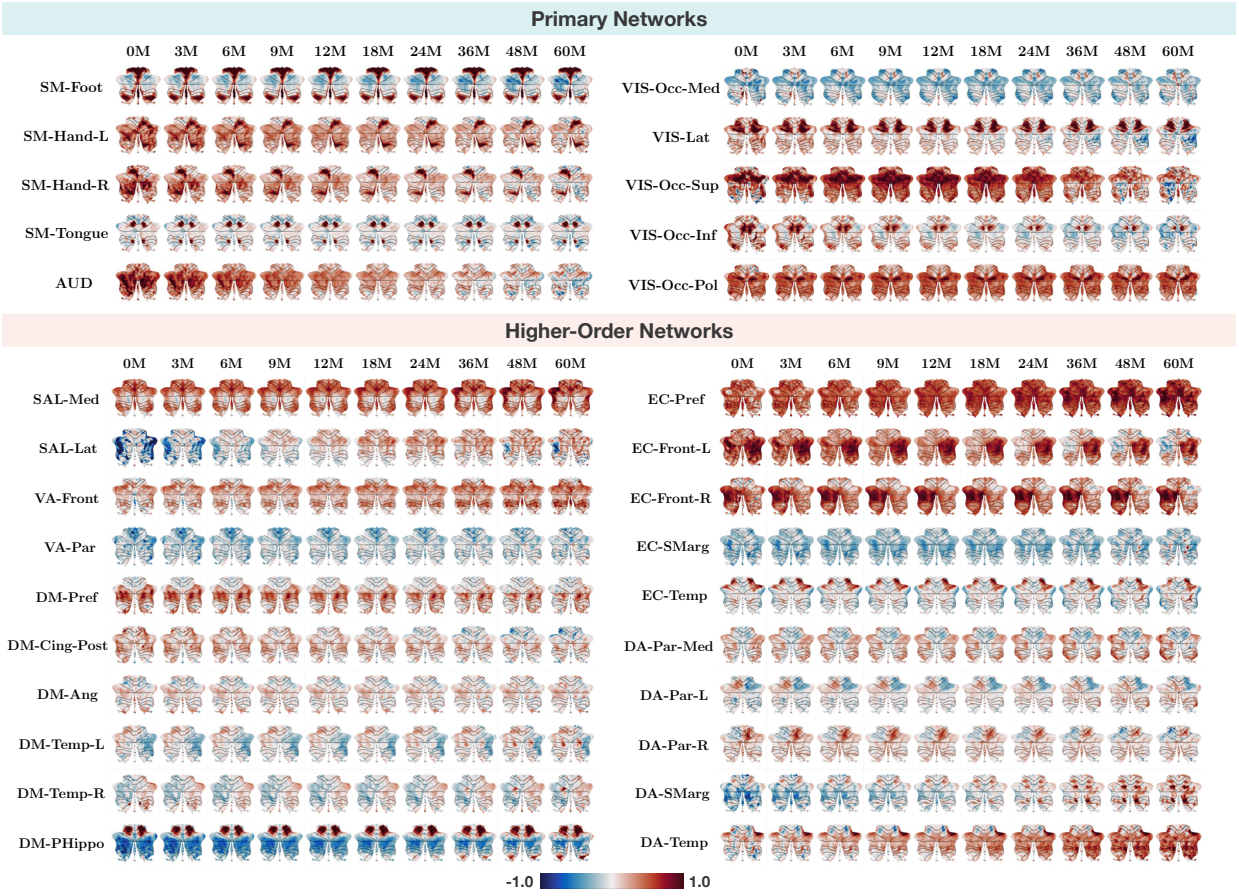

Fig. S5 | Cerebellar functional maps from birth to 60 months for male children. Spatiotemporal patterns of cerebellocortical connectivity (z-transformed) between the cerebellum and each RSN during early childhood in males. Values beyond −1.0 to 1.0 are capped for clarity.

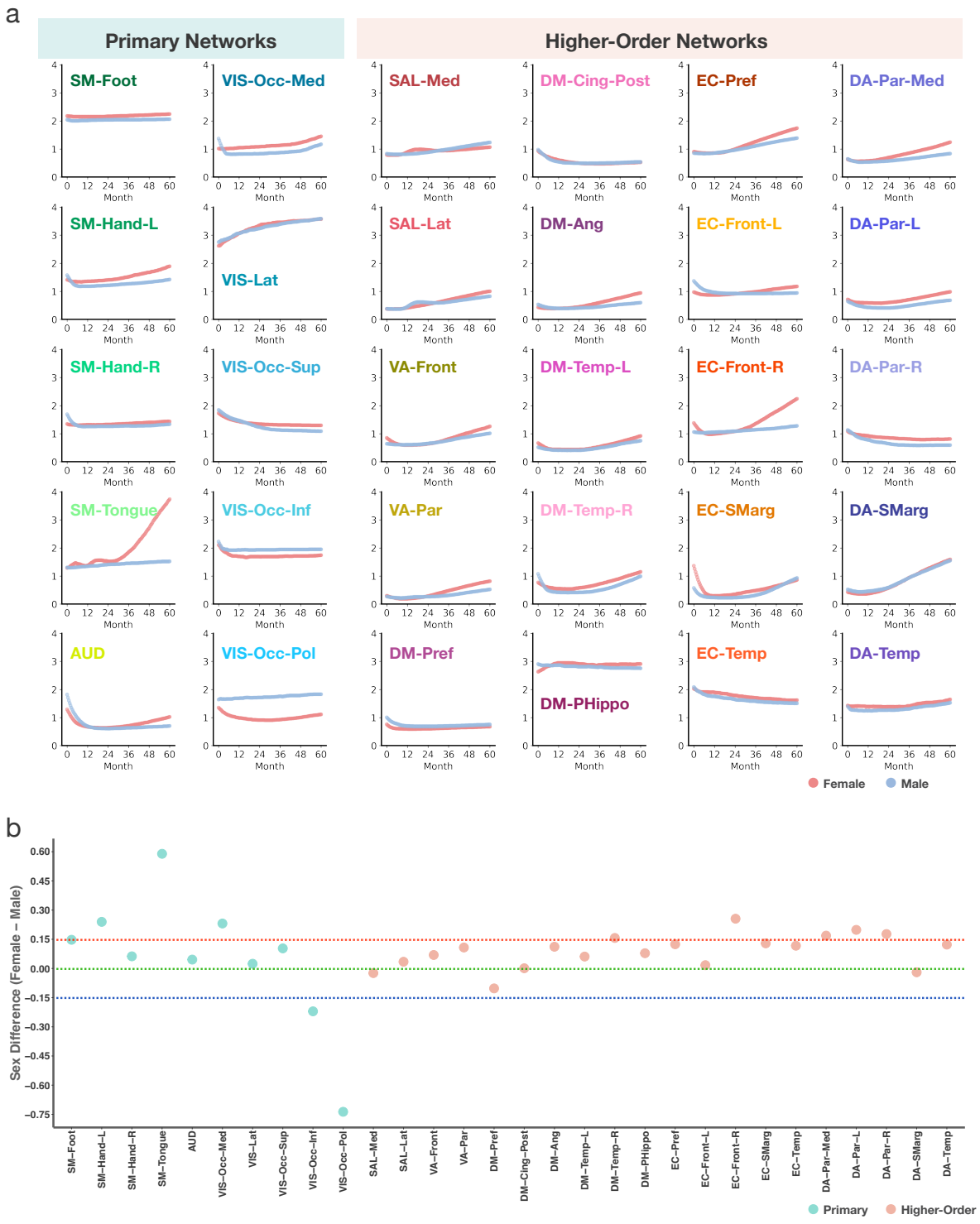

Fig. S6 | Developmental trends of cerebellocerebral connectivity in female and male children. **a**, Trajectories of the 99th percentile cerebellar connectivity (z-transformed) with each RSN over time across female and male children. **b**, Mean sex differences in cerebellar connectivity with each RSN, calculated at biweekly intervals from 0 to 60 months. Values above the red dashed line indicate substantially higher connectivity in females compared with males, values around the green dashed line indicate negligible or minimal differences in connectivity between females and males, and values below the blue dashed line indicate substantially lower connectivity in females compared with males.

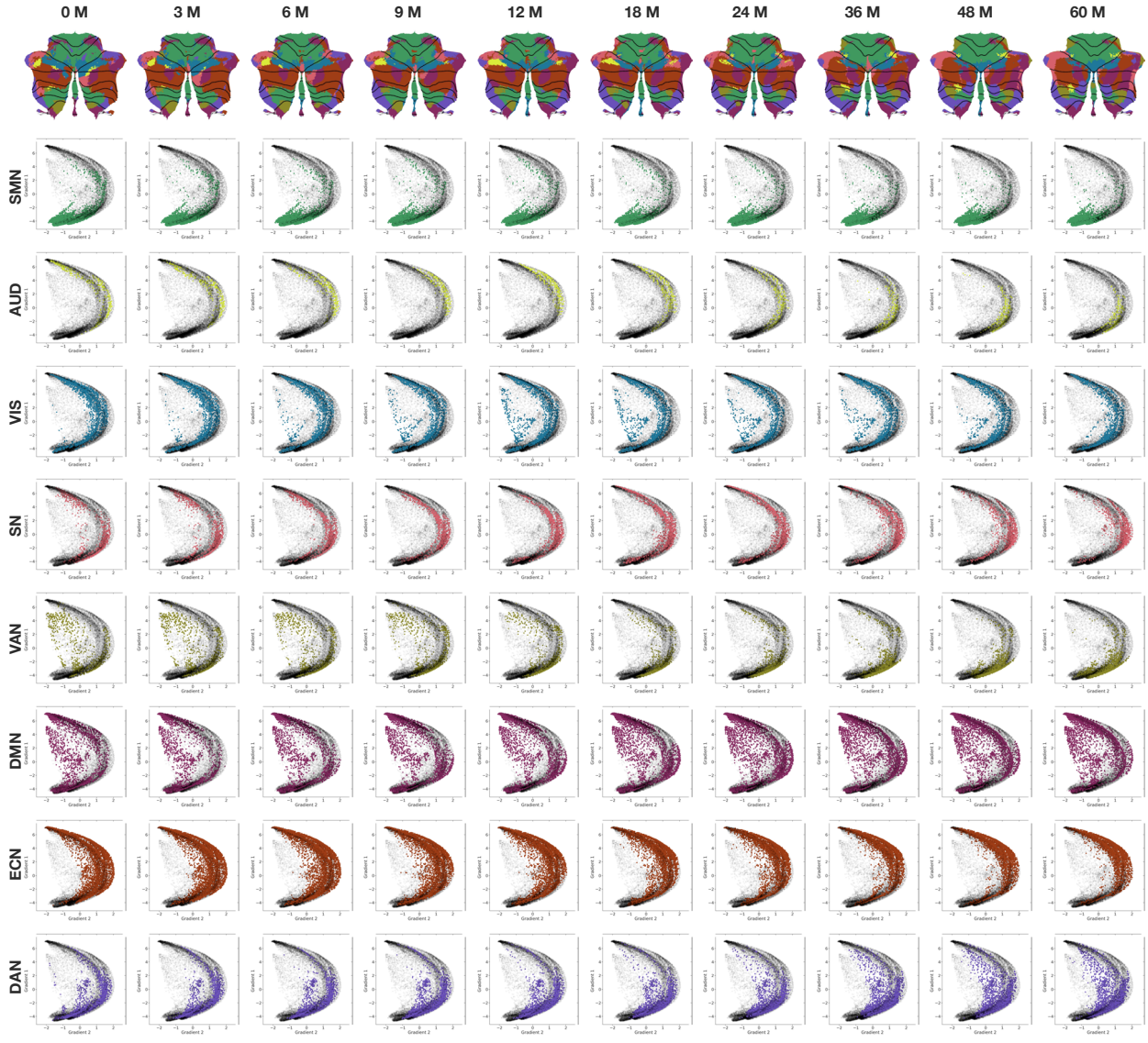

Fig. S7 | Gradient mapping of each large-scale network in children of both sexes over time.

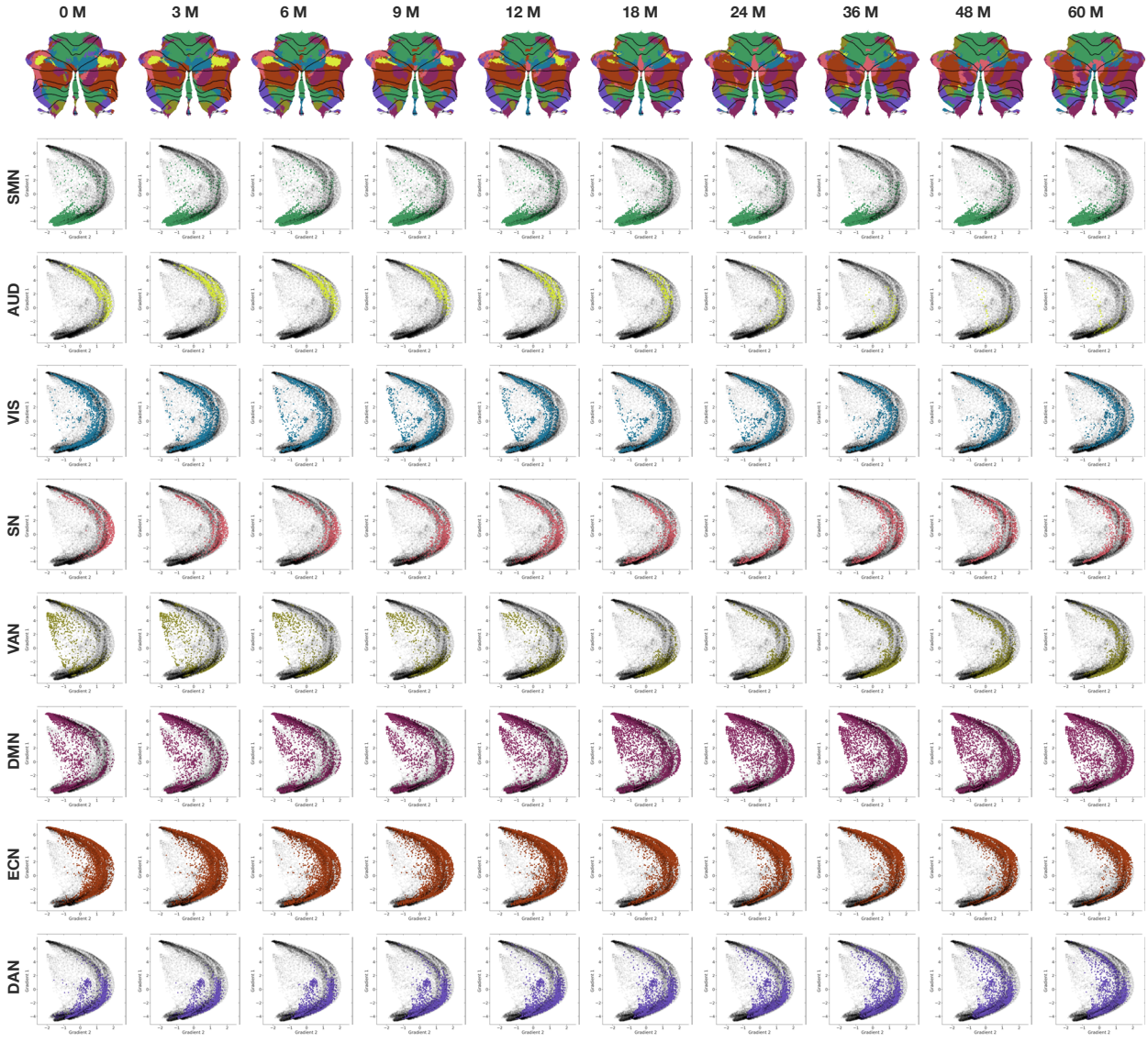

Fig. S8 | Gradient mapping of each large-scale network in female children over time.

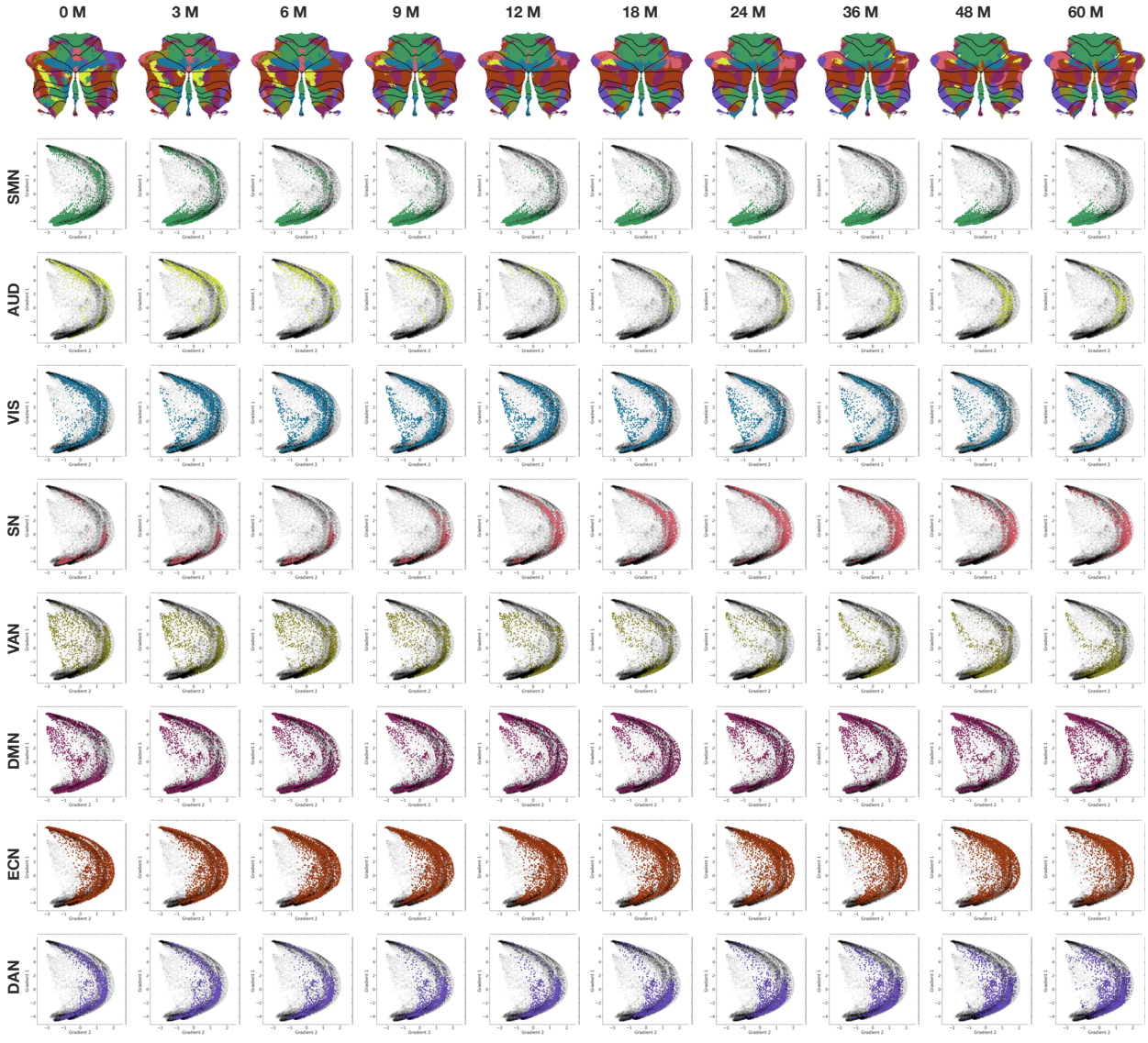

Fig. S9 | Gradient mapping of each large-scale network in male children over time.